Research Article

Quantifying Knowledge Production Efficiency with Thermodynamics: A Data Driven Study of Scientific Concepts

Artem Chumachenko[1], **Brett Buttliere**[2]

1. Science Studies Lab, University of Warsaw, Poland; 2. University of Warsaw, Poland

We present a data-driven thermodynamic framework for analyzing how scientific concepts evolve as open, non-equilibrium systems coupled to an informational environment. Each concept is modeled as a grand-canonical ensemble whose empirical frequency distribution follows a generalized Boltzmann form derived from the Maximum Entropy principle. Using large-scale data from more than 500,000 physics papers (about 13,000 concepts, 2000–2018), we reconstruct temporal trajectories of key thermodynamic observables such as temperature, entropy, free energy, and residual entropy, and identify three characteristic regimes of concept dynamics: stochastic, non-equilibrium, and equilibrium. The analysis reveals an empirical stability plateau in the ratio between entropy and effective information energy, with mature concepts clustering around a characteristic value. This behaviour reflects a finite-size scaling constraint on the accessible informational phase space, and marks the transition to a buffered regime in which entropy production and information dissipation become balanced. In this regime, well-established concepts behave as effective thermodynamic reservoirs that stabilize the informational environment of their field. Using the Hatano–Sasa decomposition of irreversible work, we introduce efficiency measures that separate steady maintenance dissipation from adaptive reorganization costs. Together, these quantities provide a unified, thermodynamically consistent description of how scientific concepts emerge, stabilize, and reorganize under finite informational capacity, offering new insight into the statistical mechanics of knowledge production.

Corresponding author: Artem Chumachenko, a.chumachenko@uw.edu.pl

 doi.org/10.32388/UM6NLZ.3

1. Introduction

Entropy occupies a central position in both physics and information theory as a measure of multiplicity, uncertainty, and disorder. Since the work of Boltzmann and Gibbs, thermodynamic entropy has quantified the number of microscopic configurations compatible with a macroscopic state. Shannon [1] extended this concept to symbolic communication, defining information entropy as a measure of uncertainty within message ensembles. Jaynes [2] later showed that the two are not merely analogous but formally connected: statistical mechanics can be reformulated as an inference procedure based on the Maximum Entropy (MaxEnt) principle, where physical laws provide the relevant macroscopic constraints. This insight laid the foundation of modern statistical inference and has inspired extensive research linking informational and thermodynamic quantities across physics, chemistry, biology, and cognitive systems [3][4][5].

However, the relationship between thermodynamic and information-theoretic entropy remains a topic of conceptual debate [6][7]. Thermodynamic entropy, rooted in classical physics, measures the number of microstates consistent with given macroscopic observables, while Shannon entropy quantifies uncertainty in a probability distribution. Their mathematical forms are identical, but their physical interpretation aligns only when the probabilities in the Shannon expression correspond to the MaxEnt distribution, the least biased estimate consistent with known constraints such as average energy or particle number. In this sense, Jaynes' equivalence is conditional, not absolute. As several authors emphasize [8][9], entropy should not be regarded as an intrinsic property of a system but as a measure relative to the observer's description; Caticha succinctly notes that "*entropy is fundamentally tied to our method of observation and description, rather than being an intrinsic property of the system under study*." Entropy therefore depends on the descriptive level—microstate, mesostate, or macrostate—and differences between these levels quantify the additional information required to uniquely specify a system. Gao et al. [10] further formalized this connection, showing that thermodynamic and Shannon entropy coincide precisely when the underlying probability distribution assumes a generalized Boltzmann form. This result provides the theoretical foundation for applying thermodynamic reasoning to information-theoretic and cognitive systems described via MaxEnt methods.

An essential physical understanding that supports this correspondence is the Landauer principle, which establishes the minimal energetic cost of information processing [11]. According to this principle, any logically irreversible operation, such as erasing a bit of information, must be accompanied by a corresponding increase in entropy and dissipation of at least $Q = k_B T ln2$ of heat to the environment.

This result unifies computation and thermodynamics by asserting that the information has an unavoidable physical embodiment. Together with Brillouin's notion of negentropy[12], Landauer's principle grounds the generalized second law of thermodynamics, in which information and energy are jointly conserved: the decrease in informational entropy within a system must be compensated by an equal or greater increase in thermodynamic entropy elsewhere [13]. In the context of knowledge production, this principle implies that the acquisition or refinement of knowledge, understood as a reduction of uncertainty, necessarily involves a corresponding expenditure of energy, effort or cognitive work.

Within this framework, scientific communication can be viewed as an open infodynamic system: one in which symbolic entities like scientific concepts, rather than particles, interact, transform, and organize under constraints of limited attention and transmission capacity. In the digital era, this collective system of knowledge is embodied in a vast and continuously evolving corpus of publications amenable to computational analysis. By extracting its ontology, a structured set of scientific concepts, and examining their statistical behavior in texts, we can represent science as a dynamic network of interacting information units[14][15]. Each concept, operationally defined as an n gram encoding a scientific notion, model, or process (e.g. *energy*, *mass*, or *quantum Hall effect*), reflects a local degree of informational activity within the global system.

Empirical studies reveal that word and concept frequencies in scientific corpora follow power-law distributions, whereas co-citation and co-occurrence networks exhibit small-world and hierarchical structures. These regularities suggest that the production and diffusion of scientific knowledge may follow principles analogous to entropy maximization and energy redistribution in physical systems. Just as classical thermodynamics provided a framework for optimizing energy and work during the industrial revolution, a thermodynamic perspective on information may illuminate the organization and efficiency of knowledge in the digital age. Conceptualizing scientific communication as a collection of statistical-mechanical ensembles of evolving informational states enables a rigorous and quantitative analysis of its structure, dynamics, and emergent thermodynamic behavior.

Despite the growing number of studies exploring thermodynamic analogies in social and informational systems, a clear theoretical and methodological gap remains. Existing models, such as the thermodynamic principles of social collaboration proposed by Peng [16] offer valuable insights but operate at a binary or coarse-grained level of description, where the presence or absence of a *logical particle* in the message defines the state of the system. This binary approach simplifies empirical implementation but collapses the internal heterogeneity of concept usage, implicitly fixing the number of such "particles" and thus

constraining the system to a canonical-like regime. As a result, it cannot capture the open-system fluctuations, mesoscopic structure, or connections to thermodynamic potentials necessary for a complete description of information dynamics. More generally, the literature lacks a grand-canonical, frequency-resolved framework for modeling scientific concepts as open thermodynamic systems, one that explicitly derives their equilibrium reference states from the MaxEnt principle and links these to measurable thermodynamic quantities such as temperature, chemical potential, free energy, and heat capacity.

The present work addresses this gap by developing a thermodynamic framework that treats each scientific concept as an open grand-canonical ensemble that exchanges 'logical particles', its textual mentions, with a document reservoir. This approach extends previous binary models by introducing a frequency-resolved, open-system formalism grounded in MaxEnt and consistent with the Landauer limit and the generalized second law. In this framework, the empirical distribution of the concept frequencies defines the mesoscopic structure of the system, while the corresponding equilibrium distribution, shown to take the form of a generalized Boltzmann law, represents its macrostate. By comparing empirical, non-equilibrium states with their equilibrium projections, we can quantify entropy production, information exchange, and thermodynamic efficiency in knowledge production. This enables a unified and physically interpretable description of how scientific concepts evolve, stabilize, and interact within the collective thermodynamic landscape of scientific communication.

2. Materials and Methods

2.1. Database description

For our analysis, we used a corpus of 451,524 English-language research articles from the High Energy Physics and Astronomy sections of `arXiv`, spanning the period 2000–2018. Each record contains the full text of the document as well as standard bibliographic metadata (title, authors, publication date, and abstract). In addition, each document was annotated with term-frequency counts for 13,945 scientific concepts drawn from a curated domain ontology[14][17][18]. All data processing and thermodynamic parameter estimation were performed on a Google Cloud Linux virtual machine using *Wolfram Mathematica* 14.3 in combination with a *MySQL* backend for efficient large-scale storage and querying.

This corpus and closely related variants have previously been examined in the context of concept network structure, innovation emergence, and topic extraction dynamics. Previous studies have used network embedding techniques to trace the emergence of scientific innovations within the arXiv concept co-

occurrence network [19]; applied entropic selection methods to identify latent topical organization in scientific corpora [20]; and analyzed empirical scaling properties and growth patterns of scientific concept networks [21]. While these works focus primarily on structural and network-theoretic characterizations, the present study develops a thermodynamic framework for the same concept usage data, providing a complementary description in terms of residual entropy, free energy, and nonequilibrium work associated with semantic evolution.

2.2. Thermodynamic framework

To formalize our model, we consider the scientific concept c and define its empirical support at time t as the collection of relevant documents that contain at least one mention of the concept. The number of such documents is denoted $N_c(t)$ among the total number of $N_D > N_c$ documents in a corpora. If no further information is known beyond whether a concept appears in the document or not (Peng et al. binary approach[16]), then a uniform probability $1/N_c(t)$ can be assigned to each document. This yields a maximum entropy value of $\ln N_c(t)$ per document, representing the highest possible uncertainty under this minimal description[22][23]. In this representation, each document is associated with a single indistinguishable *microstate* of a concept.

More detailed information on a concept state arises from the in-text term frequency analysis, where each frequency class $k \in \mathbb{Z}^+$ defines a *mesostate* – a coarse-grained representation of the underlying microstates of individual concept mentions [24]. The corresponding empirical probability, $p(k,t) = N_c(k,t)/N_c(t)$ is proportional to the number $N_c(k,t)$ of documents that mention the concept c exactly k times at time t. The Shannon entropy of this mesoscopic description:

$$S(t) = -\sum_{k=1}^{\max(k)} p(k,t) \ln p(k,t), \tag{1}$$

quantifies the uncertainty or diversity of concept usage across documents. Because $S(t)$ reflects structural organization rather than pure randomness, it is typically smaller than the maximal value $\ln N_c(t)$ corresponding to uniform ignorance unless it is a new concept.

In the early stage of its appearance, a concept is supported by only a small number of documents, and its mesostate $p(k,t)$ is correspondingly sparse and almost identical to its microstate configuration. In this regime, the dynamics of $p(k,t)$ is governed primarily by *stochastic accumulation* of new mentions, driven by heterogeneous research events rather than by stable semantic context. Formally, the evolution can be described by a master equation of the form

$$\frac{d}{dt}p(k,t) = \sum_{k'}\Big[W_{k'\to k}(t)\,p(k',t) - W_{k\to k'}(t)\,p(k,t)\Big], \tag{2}$$

where $W_{k\to k'}(t)$ denote effective transition rates reflecting how documents accumulate additional mentions of the concept. The concept behaves as a *nascent nonequilibrium entity*, whose structure is shaped by contingent research activity rather than by a coherent semantic environment.

As the concept accumulates sufficient usage across documents, the empirical distribution $p(k,t)$ stabilizes and develops a well-defined heavy-tailed form. This enables a power–exponential fit $p(k,t) \propto k^{-\beta_t} e^{-\lambda_t k}$, defining the concept's *instantaneous fixed point* (IFP) [24]. The power law $k^{-\beta_t}$ is responsible for the fat tail of the distribution, while the cutoff $e^{-\lambda_t k}$ for the finite size of the frequency band $\{k\}$. The values of these coefficients can be obtained from the maximization of S under two empirical constraints: the mean frequency $\langle k\rangle_p$ and the logarithmic moment $\langle \ln k\rangle_p$, both computed from the observed empirical distribution $p(k,t)$. This constrained maximization yields:

$$\pi(k,t;\beta,\lambda) = \frac{1}{Z}\,\frac{e^{-\lambda k}}{k^{\beta}}, \qquad Z = \sum_{k=1}^{\infty}\frac{e^{-\lambda k}}{k^{\beta}} = Li_{\beta}(e^{-\lambda}), \tag{3}$$

where Z is the normalization constant expressed through the polylogarithm function $Li_{\beta}(e^{-\lambda})$, and $\beta, \lambda > 0$ are Lagrange multipliers determined by:

$$\langle k\rangle_p = \langle k\rangle_\pi = \frac{Li_{\beta-1}(e^{-\lambda})}{Li_{\beta}(e^{-\lambda})}, \qquad \langle \ln k\rangle_p = \langle \ln k\rangle_\pi = -\frac{\partial_\beta Li_{\beta}(e^{-\lambda})}{Li_{\beta}(e^{-\lambda})}. \tag{4}$$

The entropy of the resulting macrostate then follows as [20]:

$$S_{\text{macro}} = -\sum_{k=1}^{\max(k)} \pi(k,t)\ln\pi(k,t) \tag{5}$$

$$= \ln Z + \beta\left(\langle \ln k\rangle_p + \frac{\lambda}{\beta}\langle k\rangle_p\right). \tag{6}$$

Following the standard approach in statistical mechanics, the instantaneous macrostate entropy S_{macro} is mapped onto the entropy of the open thermodynamic system S_{therm} through the relation[25]:

$$S_{\text{therm}} = k_B S_{\text{macro}} = k_B\left(\ln Z + \beta U - \mu\beta N\right), \tag{7}$$

where k_B is the Boltzmann constant (set to unity throughout), $\beta = 1/T$ is the inverse temperature, $U = \langle \ln k\rangle_{p,\pi}$ represents the internal energy of the system, $\mu = -\lambda/\beta$ is the chemical potential and $N = \langle k\rangle_{p,\pi}$ is the average number of logical particles. The normalization constant Z now serves as the grand partition function of the ensemble.

The thermodynamic interpretation of Eq. (7) is justified by recognizing that the distribution $\pi(k, t; \beta, \lambda)$ is a special case of the generalized Boltzmann distribution[10]. In this formulation, a scientific concept is modeled as an open thermodynamic system composed of discrete information units, or logical particles, each representing a single in-text mention within a scientific publication, which remains open to the inflow or depletion of logical particles from the surrounding document reservoir. Documents serve as heterogeneous containers that accommodate varying numbers of such particles. In this representation, the microstates correspond to distinct document-level realizations of the concept, while the ensemble averages define its macroscopic informational state specified by the variables (U, N, T, μ). Together, these quantities describe a macrostate coarsegrained configuration of the concept frequency mentions at a given moment, analogous to the equilibrium state of an open thermodynamic system.

Importantly, while π describes such an instantaneous equilibrium configuration under the prevailing constraints, the empirical distribution $p(k, t)$ generally deviates from it. This deviation quantifies the degree to which the current informational structure of the concept differs from its IFP, reflecting the fact that concepts evolve as *nonequilibrium systems* continuously shaped by the expanding and reorganizing corpus. Within this framework, the departure from equilibrium can be expressed as residual entropy $R(t)$ or *athermality*[26][27], which measures the information required to specify the system's nonequilibrium state relative to its maximum-entropy reference. This formulation naturally extends the thermodynamic description to the dynamical regime, enabling the consistent definition of entropy production, free energy dissipation, and irreversible informational work in the evolution of concept usage. In this sense, the informational thermodynamics of concepts captures how structured knowledge emerges, stabilizes, and dissipates within the evolving scientific corpus.

2.3. Residual Entropy and Free Energy

We refer to a concept as being in *equilibrium* – more precisely, in a stationary state – when its empirical mesoscopic entropy S coincides with the corresponding maximum entropy value S_{macro}. In this limit, the macroscopic descriptors (U, N, T, μ) cease to evolve in time, and the informational structure of the concept becomes effectively stabilized.

The trajectory of a concept toward such a stationary state can be understood geometrically. The family of IFP distributions $\{\pi(\beta, \lambda)\}$ forms a smooth statistical manifold equipped with the Fisher information metric [28][29]. The *thermodynamic length* of the trajectory of a concept in this manifold quantifies the cumulative amount of irreversible dissipation required to traverse it. Shorter (geodesic) paths correspond

to evolution driven by minimal dissipation as for the equilibrium concepts, whereas longer paths signal sustained nonequilibrium reorganization or repeated contextual shifts more relevant for the concepts that represent a novel ideas.

Equilibrated concepts are typically highly generic and foundational terms that appear broadly in many documents and contexts. In the high–energy physics corpus, examples include terms such as *particle*, *field*, *entropy*, etc. Their frequency distributions already maximize Shannon entropy given their moment constraints, yielding $R \approx 0$ and making them behave as stable and statistically balanced *informational reservoirs*. Such concepts form the core equilibrium background against which more specialized concepts evolve.

A collection of such equilibrated basic concepts forms *core* for any topic – a locally stable subsystem whose collective state can be characterized by an effective temperature T_{ref}. This temperature reflects the average informational dispersion within the core and defines a local *thermal bath* for other related, dynamically evolving concepts. For each non-equilibrium concept, the surrounding topic core provides a thermodynamic reference temperature, analogous to the solvent in the Rao–Esposito formulation of chemical reaction networks [30]. Its own IFP state temperature T_c, as well as other thermodynamic parameters, may differ from T_{core}, reflecting the concept's informational distance from the nearest equilibrated (basic) concepts. Concepts in this regime populate the *topic periphery*, where residual entropy and temperature deviations indicate ongoing semantic innovation and structural reorganization. These concepts are still adapting to changing semantic and disciplinary environments, reflecting their active role in the dynamic evolution of scientific knowledge. Representing emerging or specialized terms, such non-equilibrium concepts therefore carry a higher *reactive potential* (the ability to perform work), which we quantify below. The geometric and topological properties of the resulting core–periphery structure, including its induced information curvature and metric deformation of the informational space, will be analyzed in detail in a forthcoming study [31].

The information required to specify a nonequilibrium structure of the concept with respect to its IFP baseline is quantified by the *residual entropy*:

$$R(t) = S_{\mathrm{IFP}}(t) - S(t) = D_{\mathrm{KL}}(p(t) \,\|\, \pi(t)) = \sum_k p(k,t) \ln \frac{p(k,t)}{\pi(k,t)} \geq 0, \tag{8}$$

which is the Kullback–Leibler divergence between the empirical mesostate p_c and its corresponding instantaneous macrostate π [20]. In thermodynamic terms, R represents the information content necessary to characterize the system's deviation from its IFP configuration at a given average energy

U and the number of particles N per document, and measures the effective *information capacity* or internal organization of the system[32][33][34].

Introducing the instantaneous grand potentials for the IFP state and the mesoscopic nonequilibrium state:

$$\begin{aligned} \Phi_{\mathrm{IFP}} = &\quad U_\pi - T S_{\mathrm{macro}} - \mu N_\pi = -T \ln Z, \\ \Phi = &\quad U_p - T S - \mu N_p, \end{aligned} \tag{9}$$

taking their difference, using Eq. (4) we obtain (see also Appendix D)

$$(\Phi - \Phi_{\mathrm{IFP}})_{T,\mu} = T\, R \geq 0. \tag{10}$$

Equation (10) thus expresses a nonequilibrium Landauer-type relation: the excess grand potential (or *informational free energy*) represents the energetic cost of maintaining or reorganizing the information encoded in p_c with respect to its IFP. This relation provides a thermodynamically consistent basis for describing the *informational irreversibility* inherent in the evolution of scientific concepts: deviations from IFP (positive R) correspond to stored informational energy that must eventually dissipate as the concept stabilizes.

The temporal variation of residual entropy:

$$\Delta R = \Delta S_{\mathrm{macro}} - \Delta S = R^f - R^i,$$

quantifies the change in informational structure as the system evolves from an initial to a final state over a finite interval Δt. As the system approaches equilibrium, ΔR typically decreases, reflecting the gradual loss or redistribution of structured information according to the second law of thermodynamics. However, individual entropies S_{macro} and S need not change synchronously: both may increase or decrease together, or even evolve in opposite directions (e.g. $\Delta S_{\mathrm{macro}} < 0$ while $\Delta S > 0$). Such an asynchronous evolution reflects the adaptive balance between thermodynamic disorder and the informational organization characteristic of open, driven systems.

The associated change in the grand potential Φ quantifies the system's capacity to reorganize its informational structure. When Φ is large and positive relative to its instantaneous fixed point value Φ_{IFP}, the concept carries excess informational free energy that can drive further semantic restructuring in relation to other concepts (e.g., through emerging associations, contextual shifts, or disciplinary redefinitions). Conversely, as the system approaches its steady configuration, $\Delta(\Phi - \Phi_{\mathrm{IFP}})$ decreases, signaling a reduced potential to effect such reorganization. From Eq. 10 we find:

$$\Delta(\Phi - \Phi_{\mathrm{IFP}})_T \simeq T\, \Delta R, \tag{11}$$

where $T\,\Delta R$ reflects the internal relaxation towards the IFP manifold at constant T, in which the residual informational structure is dissipated.

2.4. Irreversible Work in a Grand–Potential Framework (Baseline: No Driving)

We first consider the case in which the instantaneous fixed point π is stationary and the thermodynamic control parameters (T, μ) remain constant. These conditions define the *non-driven regime*, in which the empirical mesostate evolve autonomously, $p \to \pi$, without any external perturbation or parameter driving.

Under these conditions, the nonequilibrium identity for the second law integrated over a finite transition reduces to the Esposito–Van den Broeck result [4] (see Appendix A):

$$W_{\mathrm{irr}} = T\,\Delta S_{\mathrm{i}} + T\,\Delta R, \tag{12}$$

where T is the (constant) system temperature and $\Delta S_i \geq 0$ is the irreversible entropy production. When π is stationary, detailed local balance implies (see Appendix B)

$$\frac{d}{dt} S_i(t) = -\frac{d}{dt} R(t),$$

which integrates to

$$\Delta S_i = -\Delta R, \qquad \Rightarrow \qquad W_{\mathrm{irr}} = 0. \tag{13}$$

Thus, for such a hypothetical transition (with $\Delta R > 0$), the residual informational structure R is entirely converted into entropy, and R acts as a Lyapunov function that governs relaxation towards the IFP manifold [35][36][37][38]. Equation (13) is also trivially satisfied when $\Delta R = 0$, i.e., when the residual information potential remains constant over the time interval Δt.

In physical systems, the case $\Delta R > 0$ corresponds to an isothermal process in which a system with fixed total energy E and particle number N relaxes toward equilibrium, such as the expansion of an ideal gas into a larger accessible volume while in contact with a thermal reservoir. The entropy increases because the available microstates become more uniformly occupied, redistributing the system's probability mass across phase space.

In the informational system studied here, logical particles have no spatial degrees of freedom, and redistribution of microstates that would lead to higher entropy is possible only when the corpus expands – when new documents introduce additional logical particles into existing or newly accessible k-channels (frequency states). In this process, both the first and logarithmic moments of the mesoscopic distribution may change, thereby modifying the corresponding IFP parameters, temperature T and chemical potential μ. Crucially, however, empirically stationary concepts maintain nearly constant values of T and μ despite

this continuous exchange of information with their environment. This regime can be interpreted as a form of *thermodynamic buffering near a critical point*.

The large response coefficients (susceptibility and heat capacity) observed for such core concepts indicate that the region near the most probable MaxEnt parameters ($\beta \simeq 3/2$, $\lambda \simeq 0$) corresponds to a parameter space that lies close to a *critical surface*, where fluctuations naturally become large. In this region, the system exhibits maximal sensitivity to perturbations, but maximal ability to absorb them – its intrinsic volatility compensates external driving, allowing T and μ to remain effectively constant. In this sense, the equilibrium core of scientific vocabulary behaves as a *buffering reservoir*: it exchanges logical particles and informational energy with the environment while preserving its intensive variables.

Analogous behavior is well known in finite physical systems operating near criticality. In the finite-size Ising model, for example, the heat capacity and magnetic susceptibility reach large but finite values near the pseudo-critical temperature, enabling the system to absorb large energy or magnetization fluctuations without a significant change in temperature or field [39][40]. Similarly, bounded open chemical reaction networks (CRNs) can maintain nearly constant internal affinities and concentrations even under external flux perturbations—an effect attributed to the large but finite response coefficients that appear near non-equilibrium steady-state bifurcations [41][42][43].

In both types of systems, finite boundaries suppress the true divergence of critical fluctuations but produce an extended region of near-constant intensive parameters—a thermodynamic buffering plateau. At the liquid–gas critical point of a van der Waals fluid, for instance, the isothermal compressibility diverges while the temperature remains fixed [44][45][46]. Thus, these physical systems act as *effective reservoirs* in criticality: their large internal capacity allows them to accommodate substantial changes in extensive variables (ΔN, ΔU) with only minimal changes in intensive ones (T, μ). In the same way, the core concepts in scientific discourse are statistically "pinned" to the critical surface, using their large intrinsic capacity to maintain a stable and self-regulating reference distribution against continual informational influx.

In this framework, the chemical potential μ—or, more precisely, the cutoff parameter λ—does not control the critical behavior itself but rather sets the *effective size of the system* in terms of the range of accessible frequency states k. Small values of λ correspond to a wider, close to power-law support of the distribution and hence to a larger "semantic volume" available to the concept. By contrast, the parameter β governs the scaling of probabilities across these states and determines the approach to criticality. Consequently, the

critical surface observed in the empirical system is primarily defined by β, while λ acts as a finite-size cutoff that regularizes the otherwise divergent behavior near the transition.

To quantify the system's sensitivity to environmental driving, we evaluated several *response coefficients*. The *heat capacities*,

$$C_\mu = \left(\frac{\partial U}{\partial T}\right)_\mu, \qquad C_N = \left(\frac{\partial U}{\partial T}\right)_N, \qquad \alpha_U = \left(\frac{\partial U}{\partial \mu}\right)_T, \tag{14}$$

characterize how the average informational energy U responds to changes in the effective temperature T at fixed chemical potential.

The *susceptibilities*,

$$\chi_T = \left(\frac{\partial N}{\partial \mu}\right)_T, \qquad \alpha_\mu = \frac{1}{N}\left(\frac{\partial N}{\partial T}\right)_\mu, \tag{15}$$

quantify how the concept's usage intensity N responds to changes in μ or in the semantic temperature of its environment.

Finally, the combined differential,

$$dE = \left(\frac{\partial E}{\partial T}\right)_\mu dT + \left(\frac{\partial E}{\partial \mu}\right)_T d\mu = C_\mu^E \, dT + \alpha_E \, d\mu, \tag{16}$$

captures the joint variations in U and N, representing the net change in the effective energy. Here, C_μ^E quantifies the thermal response of semantic energy to temperature variations, while α_E measures its coupling to the chemical potential, reflecting the sensitivity of information energy to contextual cost.

Large values of these coefficients correspond to the enhanced response typical of physical systems approaching a critical point, where the system can absorb substantial fluctuations with only minimal change in its control parameters – an informational analogue of thermodynamic buffering.

This regime stands in sharp contrast to dynamically evolving concepts discussed in the next subsection. Their IFP trajectories $(T(t), \mu(t))$ deviate from the stationary manifold, resulting in nonzero irreversible work $W_{\text{irr}} > 0$ and finite semantic adaptation effort.

2.5. Dynamic Efficiency and Non-Equilibrium Work Decomposition (driving case))

We now consider the complementary case: the dynamic regime where the instantaneous fixed point (π) evolves over time and the thermodynamic parameters (T, μ) vary under external informational driving. In this regime, the evolution of a non-equilibrium scientific concept can be represented as a trajectory through successive *non-equilibrium steady states* (NESS).The sequence of pairs $\{p_t, \pi_t\}$, where $\pi(k, t)$ locally

approximates the empirical frequency distribution $p(k,t)$, defines a coarse-grained path through the concept's informational phase space. This path characterizes how the concept's internal energy $U(t)$ and particle number $N(t)$ continuously adapt to changes in the surrounding topical environment. To quantify the efficiency of this adaptive process and the associated irreversible dissipation, we employ the Hatano–Sasa formalism[37][47], which generalizes the second law of thermodynamics to NESS transitions. This framework naturally decomposes the total entropy production (ΔS_{tot}) into parts associated with driving and maintenance.

For an open system coupled to an informational reservoir at temperature T_{ref} different from the system temperature, the total entropy production associated with a finite evolution can be decomposed into *non-adiabatic* (excess) and *adiabatic* (housekeeping) parts,

$$\Delta S_{\mathrm{tot}} = \Delta S_{\mathrm{na}} + \Delta S_{\mathrm{a}} \geq 0. \tag{17}$$

The term ΔS_{tot} represents the total irreversible entropy production estimated from mesoscopic state dynamics. The non-adiabatic term ΔS_{na} measures the dissipation associated with changes in the IFP parameters, that is, with the structural or contextual adaptation of the concept. The adiabatic term ΔS_{a} quantifies the steady "housekeeping" dissipation required to maintain the system's nonequilibrium structure (R) even under fixed environmental conditions. In discrete form, this decomposition is implemented by evaluating the Hatano–Sasa excess functional[47]

$$\widehat{Y}_{t\to t+1} = \sum_{k} p_t(k)\, \ln \frac{\pi_t(k)}{\pi_{t+1}(k)},$$

and the residual entropy change $\Delta R = D_{\mathrm{KL}}(p_{t+1}\|\pi_{t+1}) - D_{\mathrm{KL}}(p_t\|\pi_t)$. Their combination yields the non-adiabatic entropy production,

$$\Delta S_{\mathrm{na}} = \Delta R + \sum_{t} \widehat{Y}_{t\to t+1}, \qquad \Delta S_{\mathrm{a}} = \Delta S_{\mathrm{tot}} - \Delta S_{\mathrm{na}},$$

where D_{KL}, as before, denotes the Kullback–Leibler divergence between the empirical and IFP states.

The total work performed on the system along a finite evolution can be decomposed into a *reversible* (quasistatic) component and an *irreversible* (dissipative) component,

$$W_{\mathrm{tot}} = W_{\mathrm{rev}} + W_{\mathrm{irr}}. \tag{18}$$

The reversible part corresponds to the change in the grand potential evaluated on the reference IFP manifold at the bath parameters $(T_{\mathrm{ref}}, \mu_{\mathrm{ref}})$,

$$W_{\mathrm{rev}} = \Delta \Phi_{\mathrm{IFP}}^{(\mathrm{ref})} = \Big[E_{\pi_t} - T_{\mathrm{ref}}\, S_{\mathrm{macro}}(\pi_t) - \mu_{\mathrm{ref}}\, N_{\pi_t} \Big]_{t_i}^{t_f}, \tag{19}$$

and would be the only contribution in the quasistatic limit where the system remains on the IFP at all times. The remaining contribution is *irreversible work*,

$$W_{\mathrm{irr}} = W_{\mathrm{tot}} - W_{\mathrm{rev}}, \tag{20}$$

which, under isothermal conditions at T_{ref}, is directly proportional to the total entropy production,

$$W_{\mathrm{irr}} = T_{\mathrm{ref}}\, \Delta S_{\mathrm{tot}}. \tag{21}$$

In the Hatano–Sasa formalism, the total entropy production is split into non-adiabatic and adiabatic parts, $\Delta S_{\mathrm{tot}} = \Delta S_{\mathrm{na}} + \Delta S_{\mathrm{a}}$, capturing respectively the cost of structural adaptation and the steady dissipation required to maintain the nonequilibrium structure. Consequently, the irreversible work is separated into components *excess* (driving) and *housekeeping*,

$$W_{\mathrm{ex}} = T_{\mathrm{ref}}\, \Delta S_{\mathrm{na}}, \qquad W_{\mathrm{hk}} = T_{\mathrm{ref}}\, \Delta S_{\mathrm{a}}, \qquad W_{\mathrm{irr}} = W_{\mathrm{ex}} + W_{\mathrm{hk}}. \tag{22}$$

This decomposition enables us to distinguish (i) the steady energetic budget necessary to maintain a concept's existing informational structure (W_{hk}), from (ii) the additional dissipation required to reorganize or reposition the concept in semantic space (W_{ex}).

From Eq. (46) we define two complementary efficiencies:

$$\eta_{\mathrm{hk}} = \frac{W_{\mathrm{hk}}}{W_{\mathrm{tot}}} = \frac{\Delta S_{\mathrm{a}}}{\Delta S_{\mathrm{tot}}}, \quad \text{(housekeeping efficiency)},$$
$$\eta_{\mathrm{ex}} = \frac{W_{\mathrm{ex}}}{W_{\mathrm{tot}}} = \frac{\Delta S_{\mathrm{na}}}{\Delta S_{\mathrm{tot}}} = 1 - \eta_{\mathrm{hk}}, \quad \text{(driving or adaptive efficiency)}.$$

The first quantity measures the proportion of total dissipation that stabilizes the existing nonequilibrium structure, while the second reflects the share of dissipation invested in reorganizing the informational configuration of the system. A complementary indicator:

$$\rho_R = 1 - \frac{[-\Delta R]_+}{\Delta S_{\mathrm{tot}}}, \tag{23}$$

evaluates the degree to which dissipation compensates for information loss, providing a direct measure of the system's ability to maintain its residual information potential R.

The reference temperature T_{ref} defines the statistical environment in contact with the concept. Several operational choices are possible: (i) a global ontology-wide mean value $T_\star$ (e.g., the mode near $\beta \simeq 3/2,\ \mu \simeq 0$); (ii) a topic-core temperature T_{core} estimated from the ensemble of equilibrated concepts within the same topic; or (iii) an adaptive local reference $T_{\mathrm{ref}}(t)$ chosen to minimize non-adiabatic entropy production ΔS_{na} within a short temporal window. Comparing these references allows us to test whether the topic core provides a valid thermodynamic framework for the evolution of a given concept.

High values of η_{hk} identify basic stabilized concepts whose dynamics is dominated by steady maintenance of their established informational structure. Low η_{hk} values correspond to emerging or adaptive concepts for which dissipation is mainly expended in reorganizing contextual relations (high η_{ex}). As concepts approach their asymptotic equilibrium ($\beta \to 3/2,\ \mu \to 0$), both ΔR and ΔS_{i} become small, producing $W_{\mathrm{irr}} \approx 0$, consistent with spontaneous equilibration without external driving. The combined set of measures η_{hk}, η_{ex}, ρ_R therefore captures the dynamic efficiency of informational self-organization in evolving scientific knowledge systems.

3. Results

For each of the 13,945 concepts, we estimated the macrostate parameters (β, λ) in Eq. (3) in historical windows by maximum likelihood. As a cross-check, the fitted pairs were required to satisfy the moment constraints in Eq. (4) when empirical $\langle \ln k \rangle$ and $\langle k \rangle$ are computed directly from the data; fits that fail a tolerance of $< 10^{-5}$ were rejected for that window. Concepts whose mesostates were too sparse for reliable inference (distributions dominated by single mentions, k=1, implying $S = 0$) were excluded from that window; over 2000–2018 this affected 2,208 concepts, leaving 11,737 analyzed. Figure 1 displays the empirical density in the (β, λ) plane: the mass concentrates near $\lambda \in [0, 0.15]$ and $\beta \in [1, 2]$, with the mode shifting from $\beta \approx 2$ at $\lambda \approx 0$ toward $\beta \approx 1.6$ around $\lambda \approx 0.15$. Period means of β are temporally stable and close to $3/2$ ($\bar{\beta} \approx 1.51$ through 2010 and $\bar{\beta} \approx 1.61$ in 2018), consistent with heavy-tailed usage reported previously. The differences in (β, λ) are most visible in the occupancy of the information channels k. For high-support concepts, the channel mass decays approximately as a power law with non-negligible probability at large k; larger β concentrates probability in low-k channels, lowering both the mesostate entropy S and the macro entropy S_{macro}. In this regime λ is typically small, i.e., the logarithmic contribution dominates the single-particle effective energy $E(k) = \ln k - \mu k$ (recall $\mu = -\lambda/\beta$), while increasing λ enhances the effective linear part and pushes the spectrum from logarithmic-dominated toward mixed and eventually linear-dominated behavior. Empirically, mixed spectra are most frequent near $\lambda \approx 0.1$ as $\beta \to 1$, and the pure power-law limit $\lambda \to 0$ is most prevalent around $\beta \approx 2$ before declining for $\beta > 2$.

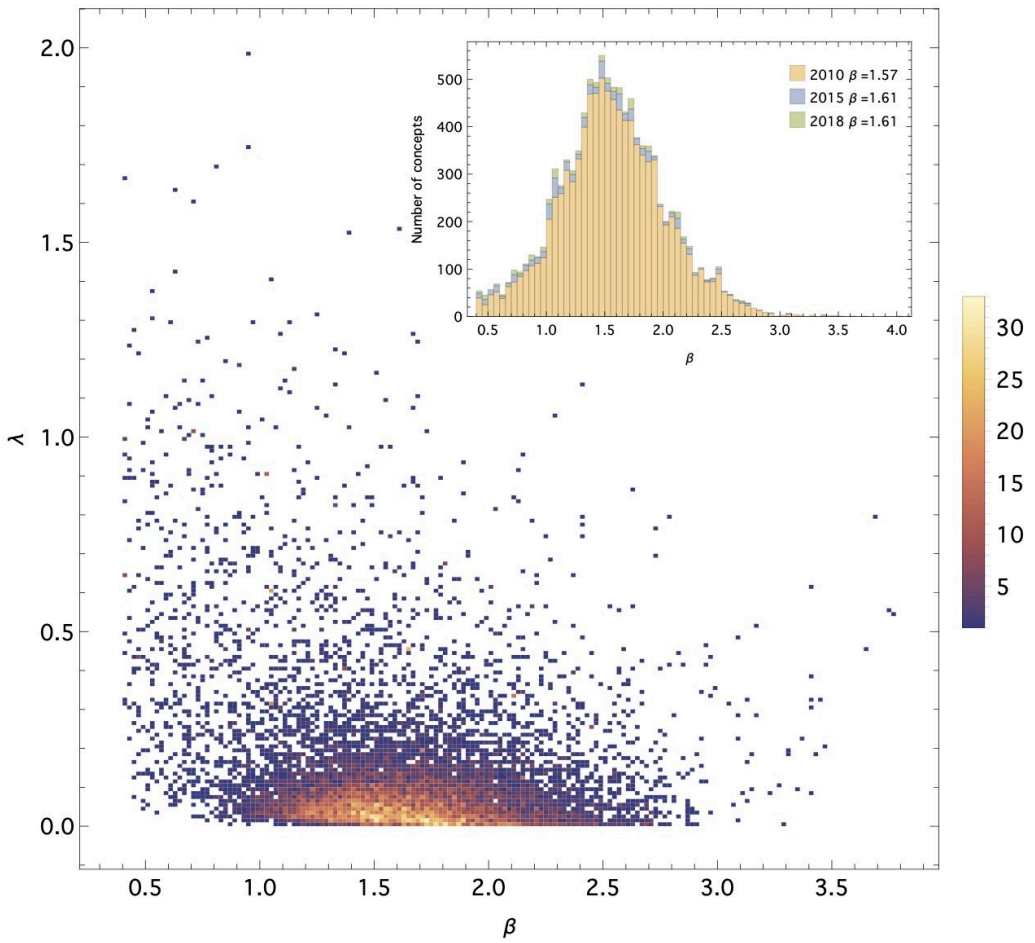

Figure 1. A heat map illustrating the distribution of macrostate parameters for 11,737 scientific concepts. The sub-figure demonstrates the distribution of inverse temperature β (where $\beta > 0.001$) and the evolution of the distribution over three time periods, beginning in 2002 and concluding in 2010, 2015, and 2018. The mean value of β, which is specified, is calculated at the end of each period.

Figure 2 arranges the macrostate parameters of the concepts by the time of their first appearance in the documents. Equilibrium-like concepts with minimal residual entropy ($R \to 0$) are overrepresented among the earliest terms, but instantaneous equilibrium is also reached by a subset of newer concepts. Not all "old" concepts are maximally entropic; many, however, exhibit quasi–power-law usage with $\lambda \to 0$. Concepts that remained thermodynamically stationary over long periods (green in Fig. 2) tend to combine near-power-law tails ($\lambda \sim 0.02$) with $R \approx 0$, saturating the Shannon–Gibbs bound under observed constraints and behave as informational reservoirs whose (U, N, T, μ) are effectively time-invariant. In this sense, they constitute the topical "bath" against which adaptive concepts evolve. The grand potential Φ (denoted A in the plots) and the inverse temperature cluster around characteristic nonzero values for

doi.org/10.32388/UM6NLZ.3

these stationary concepts, indicating a stable balance between entropic dispersal and the usage energy landscape. Concepts that equilibrated only recently share inverse temperatures close to the global mode $\beta \approx 3/2$ but often exhibit lower Φ than the long-stationary group, consistent with the reduced stored informational free energy relative to their IFP reference.

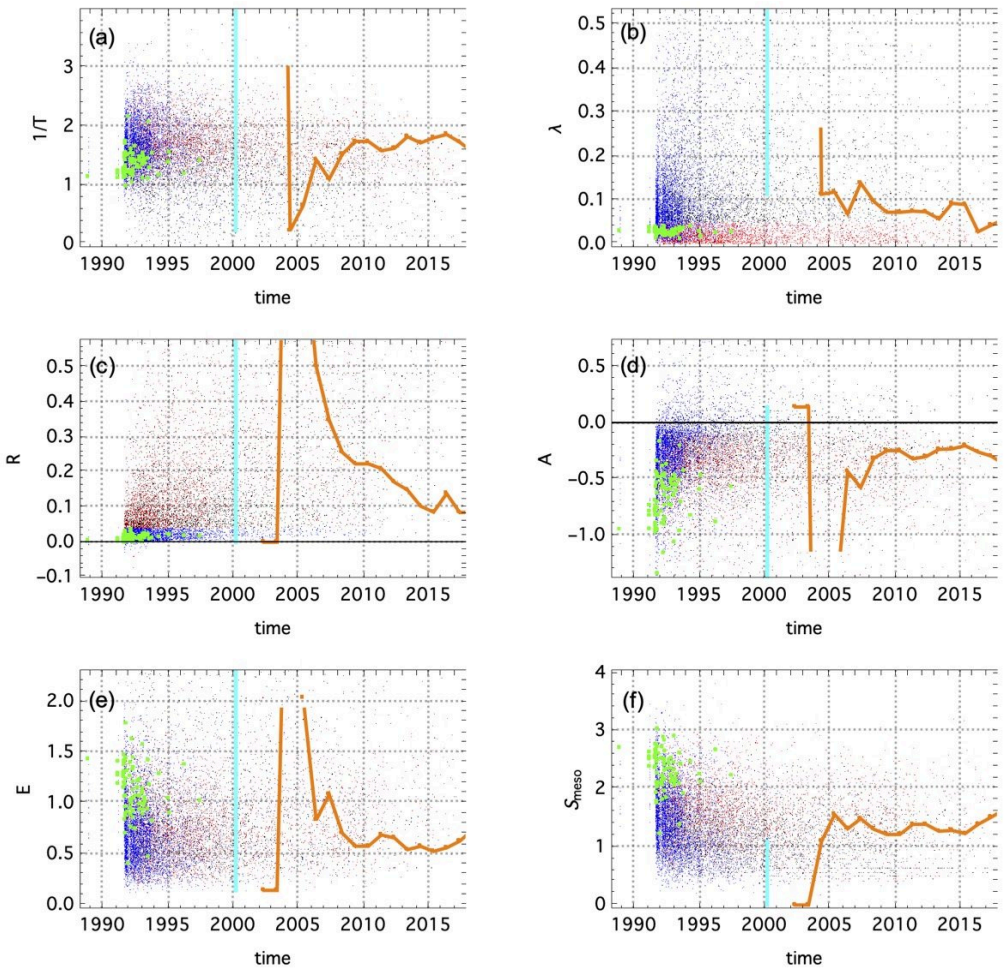

Figure 2. Thermodynamic state parameters β, λ, residual entropy R, free energy Φ (marked as A), internal energy E, and mesostate entropy S for 11,737 physical concepts, estimated from concept in-text frequency (tf) data spanning from 1991 to 2018. Concepts are ordered by the time of their first mention in the studied collection (ArXiv, which began accepting documents on August 14, 1991). Blue dots represent concepts with $R < 0.04$. Green dots indicate concepts that remained with $R < 0.04$ between 2010 and 2018. Red dots highlight concepts exhibiting a near power-law term frequency distribution ($\lambda < 0.04$), while black dots represent all other concepts. The orange line traces the state evolution of the 'Anomalous Hall effect' concept.

doi.org/10.32388/UM6NLZ.3

Figure 3 shows that document support N_c is the practical control parameter of equilibration. The concept "age" and N_c are strongly correlated, and we observe a robust threshold $N_c \gtrsim 10^3$ beyond which most concepts satisfy $R \approx 0$ and the empirical and IFP entropies coincide. As support grows, λ drifts toward zero and the term-frequency tails become more like power-law. Stationary high-support concepts are on average older and display higher S and U than other equilibrium concepts while maintaining lower Φ, indicating that over their evolutionary histories they have dissipated more informational free energy. Finally, genuinely new or rare concepts remain underdetermined within shorter windows but typically become analyzable as data accumulates; the trajectory of the 'Anomalous Hall effect' illustrates that approximately four years (2000–2004) of accumulation were required to meet the moment-matching tolerance and yield stable (β, λ) estimates.

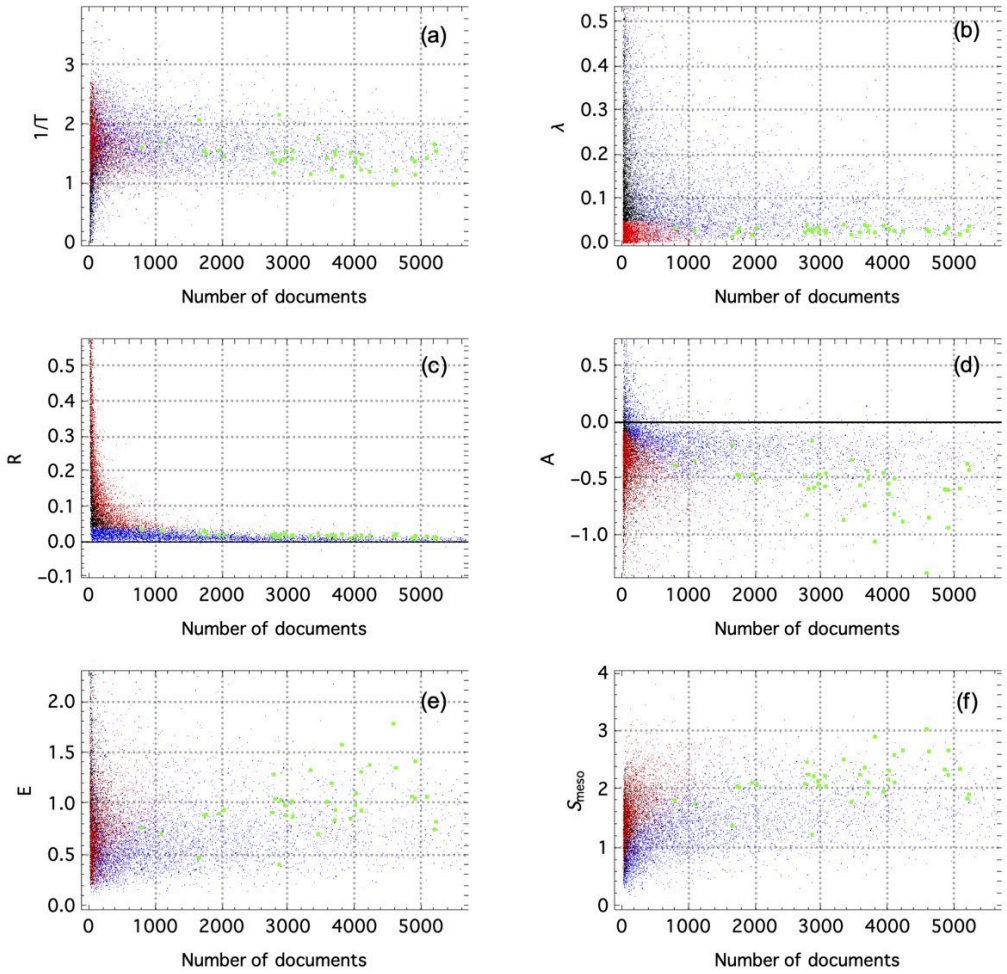

Figure 3. The concept state parameters and thermodynamic quantities as a function of the number of documents. Non-equilibrium concepts are shown in red ($\lambda < 0,04$) and black; stationary state concepts are in green, and concepts with small residual entropy R are in blue.

doi.org/10.32388/UM6NLZ.3

Together, these patterns establish a compact empirical picture that we will refine with state-diagram analyzes in the following: a concentrated landscape (β, λ) with a persistent mode near $\beta \simeq 3/2$, a progressive approach to $\lambda \to 0$ as support grows, residual entropy that decays toward zero around $N_c \sim 10^3$, and a low-Φ stationary backbone formed by high-support quasi–power-law concepts that act as informational reservoirs for the evolving periphery.

3.1. Energy-entropy diagram

To explore the organization of concept states, we mapped the ensemble of all concepts onto the energy–entropy (E–S) plane. Figure 4 show the resulting diagrams. The dashed blue curves represent the theoretical maxima of macrostate entropy S_{macro} for different fixed cut-off parameters $\lambda > 0$, computed from Eqs. (5), (4) and the corresponding energy relation. The solid blue curve denotes the limiting case of an almost pure power law ($\lambda = 0.001$). From Fig. 4 it follows that instantaneous thermodynamic equilibrium is attainable for nearly any value of λ (system size), although most concepts reach a stable equilibrium for $\lambda < 0.05$. Concepts lying close to the solid blue line therefore occupy maximal-entropy configurations for their energy, consistent with near-power-law frequency spectra.

In Fig. 4 (Right), examples of individual trajectories illustrate this behavior. Concepts such as *Diquark* and *Mass* remain in stable equilibrium for more than a decade, maintaining nearly constant internal energy and entropy. The *Diquark* concept shows a slow decline in both residual and mesostate entropy with small oscillations of temperature; on average, its free-energy changes $\Delta\Phi > 0$, indicating that it performs work in the surrounding informational environment. In contrast, the *Mass* concept preserves a small and almost constant residual entropy ($\Delta R \approx 0$) while its macrostate entropy increases slightly ($\Delta S_{\text{macro}} > 0$) at negligible change in internal energy ($\Delta E \approx 0$), implying $\Delta\Phi < 0$ and suggesting that the surrounding concepts perform work on it, gradually stabilizing its usage.

A third example trajectory, *Anomalous Hall effect*, represents the typical evolution of emerging concepts. In Fig. 4(Right), its mesostate (orange) and macrostate (red) paths show a continuous decline in both residual entropy R and effective energy E as the system relaxes. By 2018, this concept approaches its IFP at $\beta \simeq 1.5$. Earlier in its history, the parameters fluctuated strongly, but the amplitude of these variations steadily decreased towards equilibrium, in agreement with the trends visible in Fig. 2.

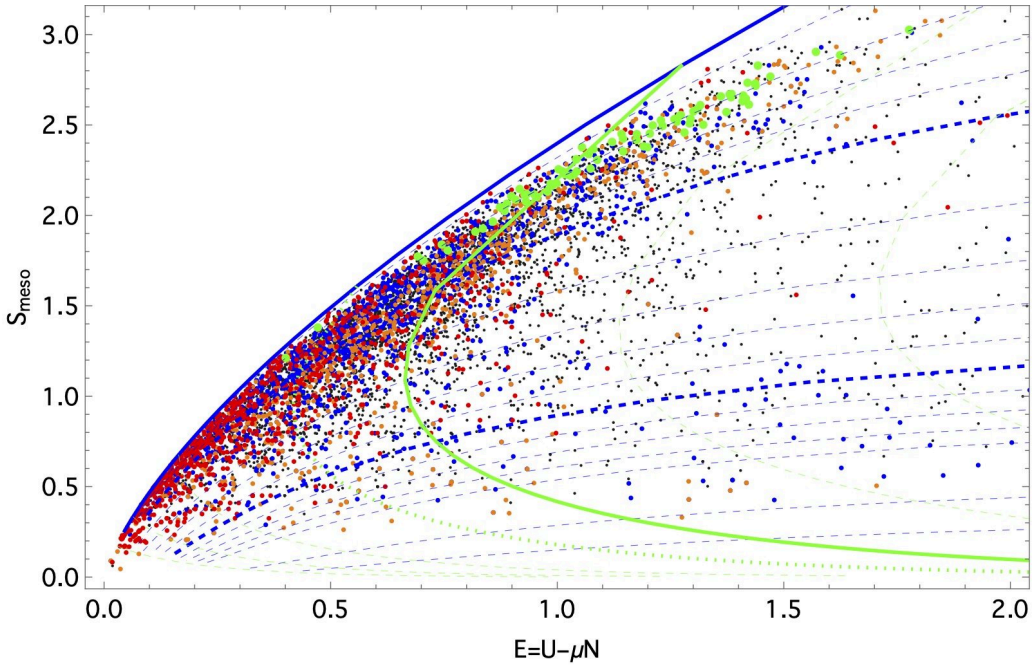

Figure 4a. Entropy–energy diagram for 11,737 physical concepts as of the end of 2018. Dots represent individual concepts: black for $R > 0.04$, blue for $R < 0.04$, and orange for $R < 0.005$.

doi.org/10.32388/UM6NLZ.3

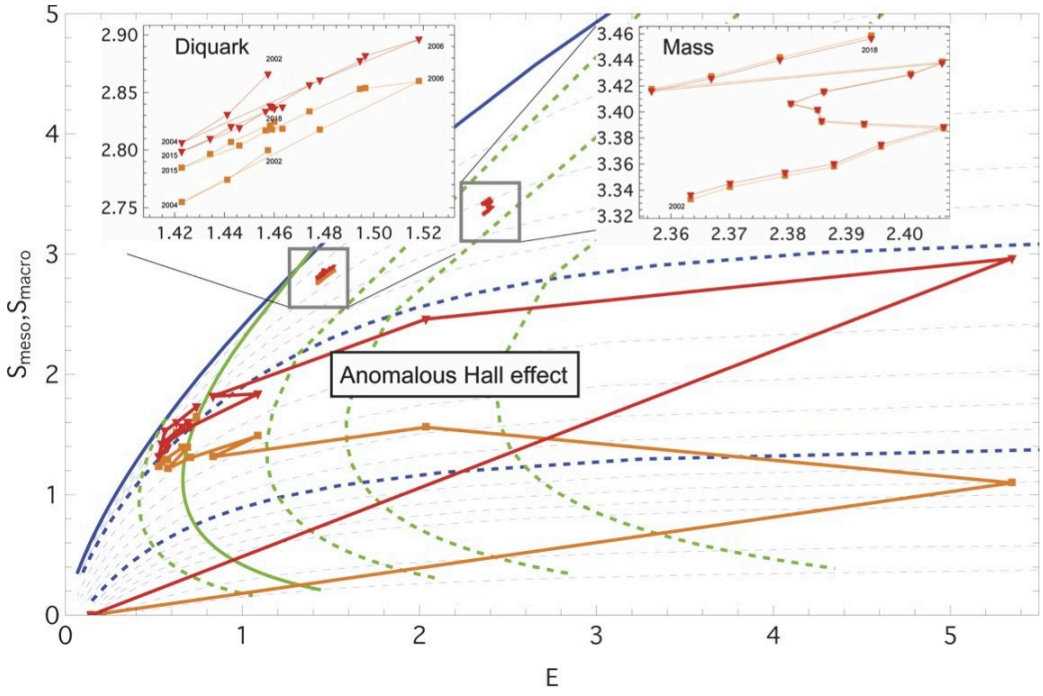

Figure 4b. Orange and red lines trace mesostate and macrostate evolution for example concepts *Diquark, Mass* and *Anomalous Hall effect*. Blue horizontal curves correspond to $S_{\text{macro}}(E(\lambda = c, \beta))$ for c range from 0.001 to 2 from top to bottom, green curves are isotherms for $\beta = \{0.5, 1, 1.5, 2\}$ from right to left, with the solid green line marking $\beta = 1.5$.

The trajectory of the *Anomalous Hall Effect* concept exemplifies the relaxation of an emerging, driven system toward the instantaneous fixed-point (IFP) manifold characterized by maximal entropy and minimal effective energy E. During its early evolution, the system operates in the *driving regime*, in which both temperature T and chemical potential μ vary strongly between consecutive intervals, indicating significant external forcing and structural adaptation. As the trajectory progresses, these fluctuations decrease, marking a transition to the *non-driving regime*, where the system's parameters stabilize and its evolution becomes effectively autonomous. At this point, the concept approaches criticality near $\beta \simeq 1.5$, where the heat capacity and susceptibility (α_μ and χ_T) reach their characteristic maxima (see Fig. 5). This behavior signifies the entry of the system into a buffered, near-critical state in which intensive variables remain nearly constant despite continued information exchange with the environment.

doi.org/10.32388/UM6NLZ.3

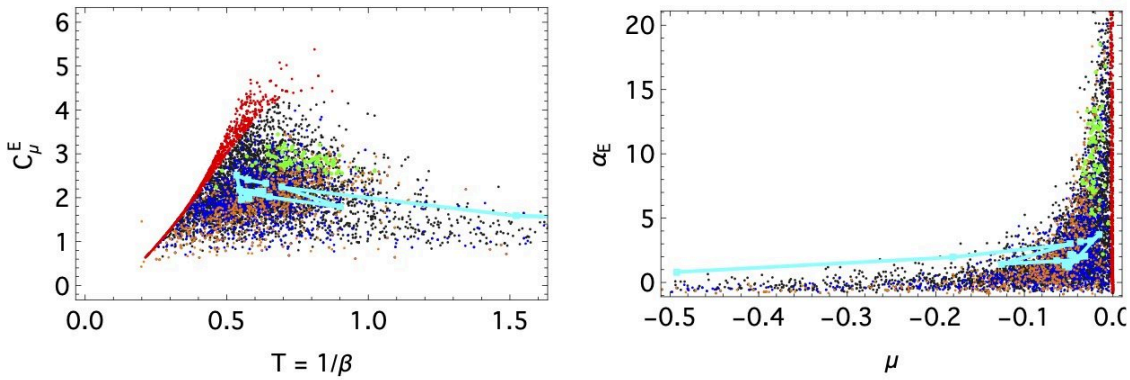

Figure 5. Heat capacity C_μ^E and susceptibility α_E diagrams. Blue dots represent concepts with $R < 0.04$, orange mark concepts with $R < 0.005$. Green dots indicate concepts that remained with $R < 0.04$ between 2000 and 2018. Red dots highlight concepts exhibiting a near power-law term frequency distribution ($\lambda < 0.04$), while black dots represent all other concepts. Cyan color mark the trajectory of *anomalous Hall effect* concept.

In Fig. 5 we show only the *effective* response pair, $C_\mu^E(T)$ and $\alpha_E(\mu)$. We focus on these quantities because they directly span the differential in Eq. 16, and, empirically, the remaining coefficients in Eqs. 14–15 exhibit the same qualitative dependence on T and μ, differing mainly in overall scale. Therefore, C_μ^E and α_E are representative of the system's thermal and chemical responses and suffice to summarize the behavior of the complete set of response functions.

Following Peng *et al.* [16], the ratio of macrostate entropy to internal energy,

$$Q^{\text{eff}} = \frac{S_{\text{macro}}}{E}, \qquad E = U - \mu N, \tag{24}$$

was originally introduced as an *entropy efficiency* and proposed to provide an alternative formulation of the second law in informational terms. In that interpretation, a system is said to "maximize its entropy efficiency," meaning it minimizes the amount of energy required to generate a given amount of entropy. While this terminology is suggestive, the notion of "efficiency" here does not correspond to the standard thermodynamic meaning of the term, since Q^{eff} does not measure a ratio of useful work to input energy.

Empirically, many equilibrium concepts cluster around the characteristic value $Q^{\text{eff}} \simeq 2$. Figure 6 (Left) displays Q^{eff} as a function of the inverse thermodynamic product $1/(TR)$, which, from Eq. 10, represents the inverse distance from equilibrium in energetic units. Figure 6 (Left) plot reveals a systematic relation between Q^{eff} and proximity to the IFP manifold for the selected concepts.

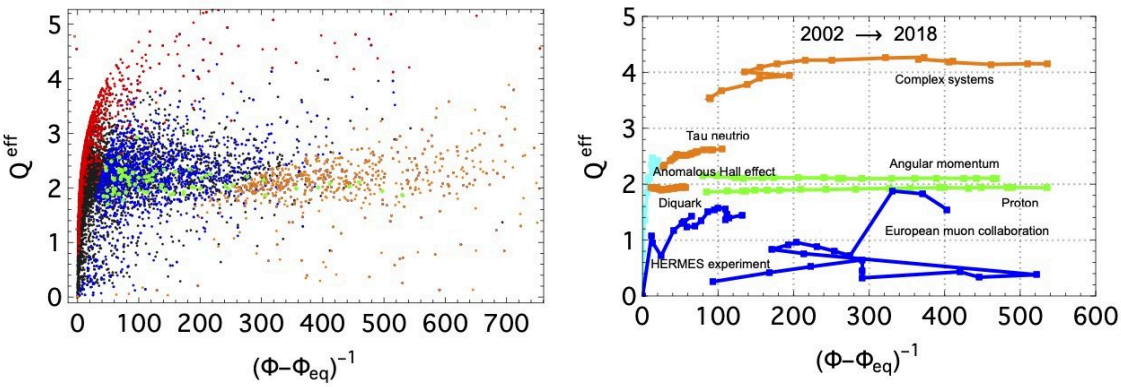

Figure 6. The entropy–energy ratio $Q^{\text{eff}} = S_{\text{meso}}/(U - \mu N)$ as a function of the inverse free-energy difference $(\Phi - \Phi_{\text{IFP}})^{-1} = 1/(TR)$. (Left) Static values computed for all concepts over the period 2002–2018. (Right) Temporal trajectories for selected examples. Green points denote stationary (equilibrium) concepts. The apparent increase of Q^{eff} toward higher values corresponds to an effective growth in system size (lower λ).

Concepts exhibiting a nearly constant entropy–energy ratio $Q^{\text{eff}} = const$ trace horizontal trajectories in the diagram (green), indicating relaxation along an iso–Q^{eff} manifold. For these cases, the residual entropy R decreases monotonically, implying positive irreversible entropy production ($\Delta S_i = -\Delta R \geq 0$) and purely dissipative relaxation toward the IFP manifold. This regime corresponds to the non-driven limit, where the instantaneous fixed point π remains stationary and no external informational work is performed.

By contrast, driven concepts display episodes where both R and Q^{eff} increase, reflecting a temporary increase in structural disorder during contextual reorganization. According to the Hatano–Sasa framework, this is fully consistent with the second law: the total entropy production

$$\Delta S_{\text{tot}} = \Delta S_i = -\Delta R + \Delta S_{\text{ex}} \geq 0$$

remains non-negative as long as the excess (driving) entropy ΔS_{ex} compensates the increase in R. Such episodes represent phases of semantic adaptation in which a concept invests additional informational work to adjust its internal distribution to a changing topical environment.

The stability plateau around $Q^{\text{eff}} \simeq 2$ marks an equilibrium-like regime of efficient dissipation, whereas excursions above or below this level correspond to adaptive transients with increased susceptibility. Concepts near this plateau behave as dynamically balanced systems—continuously driven yet thermodynamically consistent—operating close to the critical surface of the informational state space.

doi.org/10.32388/UM6NLZ.3

The right panel of Fig. 7 illustrates that the maximized version of the entropy-energy ratio TS_{macro}/E converges toward a limiting value as the effective heat capacity C_μ^E increases. Theoretical relation

$$S \lesssim \beta\beta_{\mathrm{c}}\, E, \qquad \beta_{\mathrm{c}} = \tfrac{3}{2},$$

imply $Q^{\mathrm{eff}} \leq \beta\beta_{\mathrm{c}}$, producing $Q^{\mathrm{eff}}_{\mathrm{crit}} \approx 2.25$ at the critical temperature. Empirically, most stable concepts cluster slightly below this value ($TS_{\mathrm{macro}}/E \approx 1.5$), whereas smaller or less equilibrated systems exhibit a broader dispersion. This pattern indicates that, as the effective system size or energy increases, the ratio TS_{macro}/E asymptotically approaches the predicted value reflecting a finite-size realization of the thermodynamic scaling limit.

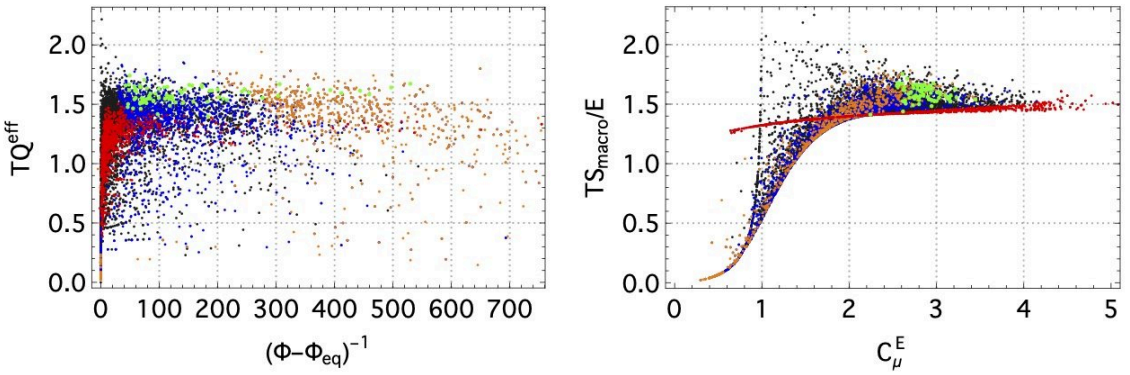

Figure 7. (Left) The dimensionless ratio $TQ^{\mathrm{eff}} = TS_{\mathrm{meso}}/(U-\mu N)$ as a function of the inverse free-energy difference $(\Phi - \Phi_{\mathrm{IFP}})^{-1} = 1/(TR)$. (Right) The maximized entropy-energy $TS_{\mathrm{macro}}/(U-\mu N$ from heat capacity C_μ^E from Eq. 16. Green points denote stationary (equilibrium) concepts. The apparent increase of Q^{eff} toward higher values corresponds to an effective growth in system size (lower λ – red dots).

This interpretation parallels well-known relations in statistical physics where entropy and energy are linearly constrained by a characteristic proportionality constant. Two classical precedents are: (i) the *Bekenstein bound*, which limits the entropy of a spatially bounded physical system by a proportionality constant multiple of its energy [48]; and (ii) *the Hagedorn scaling* in hadronic matter, where the exponential growth of the density of states produces a limiting (critical) temperature that fixes the maximal entropy per unit energy [49][50]. In the present informational framework, $\beta_{\mathrm{c}} = \frac{3}{2}$ plays the role of such a limiting proportionality constant. Concepts situated near the plateau $Q^{\mathrm{eff}} \approx 2$ thus operate close to the critical energy capacity of the system, representing a buffered regime of equilibrium-like stability, while persistent

doi.org/10.32388/UM6NLZ.3

deviations above or below this value indicate under- or over-production of entropy relative to the effective energy during adaptive reorganization.

3.2. Dissipative Regimes and Efficiency of Informational Maintenance

The decomposition introduced in Section 2.5 provides a natural basis for evaluating the efficiency and stability of evolving scientific concepts before they enter the buffered regime. In this framework, total irreversible work W_{irr} is separated into two physically interpretable components: steady *housekeeping work* W_{hk}, required to preserve the existing non-equilibrium structure, and *excess work* W_{ex}, associated with adaptive reorganization under external driving. The corresponding efficiencies from Eq. [hk_eff], η_{hk} and $\eta_{\mathrm{ex}} = 1 - \eta_{\mathrm{hk}}$, thus quantify the division of the dissipated energy between maintenance and adaptation. A complementary quantity, ρ_R from Eq. (23), measures how effectively dissipation compensates for changes in residual entropy R.

The empirical distribution of η_{hk} shown in Fig. 8, exhibits a pronounced mode near $\eta_{\mathrm{hk}} \simeq 1$, indicating that most concepts dissipate primarily to maintain their established informational structure rather than to perform adaptive reorganization. Buffered and near-critical concepts, which already operate close to equilibrium, display a wider dispersion of η_{hk} values: while the majority remain near $\eta_{\mathrm{hk}} \approx 1$, a subset exhibits significantly lower efficiencies ($\eta_{\mathrm{hk}} < 1$), corresponding to intermittent adaptation or contextual reconfiguration episodes. Concepts with nearly power-law frequency spectra ($\lambda < 0.005$) cluster strongly near $\eta_{\mathrm{hk}} \in [0.9, 1.0]$, consistent with quasi-stationary dynamics and high dissipation devoted to self-maintenance. Interestingly, the residual entropy magnitude R does not correlate directly with η_{hk}, confirming that maintenance efficiency is determined by the balance between adiabatic and non-adiabatic dissipation rather than by the absolute distance from equilibrium.

The residual–information ratio ρ_R defined in Eq. (23) quantifies how much of the total dissipation is used to counterbalance losses in the informational structure. Empirically, ρ_R assumes three characteristic values—0, 0.5, and 1—which correspond to different dynamical regimes. The plateau at $\rho_R = 1$ represents periods in which the residual information potential remains nearly constant ($\Delta R \simeq 0$), indicating efficient maintenance of the existing informational structure. The ridge at $\rho_R = 0.5$ marks a balanced exchange between information loss and entropy production (see Eq. (13)); a small dispersion around this line arises from the additional ΔS_{ex} term produced in non–equilibrium steady states (NESS) under weak driving. Finally, $\rho_R = 0$ identifies purely dissipative transitions characterized by complete structural degradation (the least populated line in Fig. 8).

For the time window (2017-2018), concepts concentrate predominantly on the $\rho_R = 0.5$ ridge ($8864/13547 \approx 65.4\%$), with a substantial fraction in $\rho_R = 1$ ($4671/13547 \approx 34.5\%$); values in $\rho_R = 0$ are rare ($12/13547 \approx 0.09\%$). All concepts with high k_{max}, which indicate a large phase space ($\lambda < 0.005$, red color), and buffered concepts (green) are located on these two ridges, while adaptive concepts (blue/orange, small R) exhibit only a narrow dispersion around $\rho_R \simeq 0.5$, consistent with partial compensation during structural reorganization.

To visualize the relationship between stability and dissipation efficiency, Figure 8 presents two joint distributions: (i) the product TQ^{eff} as a function of η_{hk}, and (ii) the entropy ratio Q^{eff} as a function of ρ_R. The first panel reveals that high housekeeping efficiency ($\eta_{\text{hk}} \gtrsim 0.9$) coincides with most equilibrium concepts, confirming that stable buffered concepts maintain both high coherence of energy entropy and steady dissipation. Lower efficiencies correspond to reduced TQ^{eff}, indicating that adaptive concepts expend more energy on structural change than on maintaining equilibrium. The second panel demonstrates that ρ_R strongly correlates with the entropy ratio: the concepts in $\rho_R = 1$ lie near the stability plateau $Q^{\text{eff}} \simeq 2$, while those in $\rho_R \approx 0.5$ deviate from it, exhibiting greater variability in their informational states. These relations reinforce the interpretation of ρ_R and η_{hk} as complementary measures of dissipative balance and structural stability.

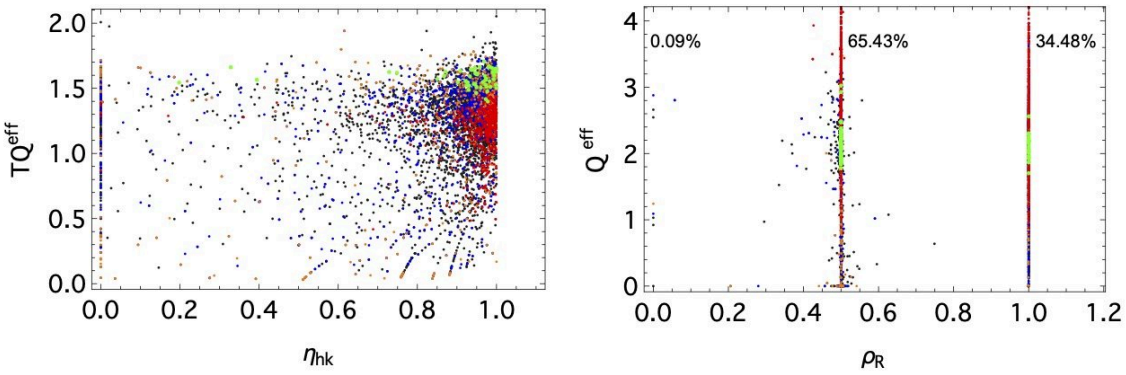

Figure 8. (Left) The product TQ^{eff} plotted against the housekeeping efficiency η_{hk} for time window 2017-2018. (Right) The entropy ratio Q^{eff} versus the residual-information ratio ρ_R. Color denotes concept class as in previous figures.

Taken together, these patterns confirm that conceptual dynamics is stratified into discrete thermodynamic modes of information processing. Stable and stationary concepts populate the *maintenance regime* ($\eta_{\text{hk}} \approx 1$, $\rho_R = 1$), where dissipation sustains informational order with minimal

adaptation. Buffered near-critical concepts occupy the *balanced regime* ($\rho_R \simeq 0.5$), characterized by reversible-like compensation between entropy production and information loss. Emergent or reorganizing concepts lie in the *adaptive regime* ($\eta_{\text{hk}} < 0.5$), where excess work drives contextual reconfiguration at the expense of higher dissipation. This tri-modal structure represents a thermodynamic taxonomy of knowledge evolution, linking stability, efficiency, and information dissipation in the self-organization of scientific concepts.

4. Discussion

The thermodynamic framework developed in this study provides a data–driven formalization of how scientific concepts evolve within the collective knowledge system. By treating concepts as open grand–canonical ensembles accepting informational energy and logical particles from their textual environment, we show that their frequency distributions conform to generalized Boltzmann statistics. This allows the introduction of measurable thermodynamic quantities such as temperature, free energy, residual entropy, and irreversible work—enabling a consistent mapping between the dynamics of concept usage and the principles of nonequilibrium thermodynamics. In contrast to previous work that invoked thermodynamic analogies only qualitatively[16], our approach derives these quantities directly from empirical distributions, providing a physically interpretable quantitative description of the evolution of knowledge.

A central finding of the analysis is that concepts exhibit three characteristic regimes of evolution: stochastic, nonequilibrium, and equilibrium. Newly emerging or weakly supported concepts behave as stochastic systems dominated by random fluctuations in usage, whose evolution is described by the master equation. As empirical support grows, concepts enter a nonequilibrium (driving) regime where their distributions acquire a power-exponential form and begin to converge toward instantaneous fixed–point (IFP) manifolds. Finally, basic concepts approach equilibrium in a non-driving regime (autonomous), characterized by constant intensive parameters (T, μ) but gradually decreasing free energy difference ($\Phi - \Phi_{IFP} = TR$). This progression mirrors the general behavior of open thermodynamic systems relaxing from driven, dissipative dynamics toward stationary states.

Empirical state diagrams reveal that the ensemble of scientific concepts self–organizes near a critical temperature $\beta_c = 3/2$ and near zero chemical potential μ, where heat capacity and susceptibility reach their maximums. This point corresponds to a transition between the exploratory and stabilized knowledge regimes and marks the beginning of *thermodynamic buffering*, a condition in which intensive variables remain nearly constant despite ongoing information updates (in U and N) from the

environment. Analogous phenomena are known in finite physical systems, such as bounded chemical reaction networks and finite–size Ising models, where large but finite response coefficients suppress true divergences while maintaining stability near criticality [51][52][53][54][55][56][57]. In this sense, the equilibrium core of scientific ontology functions as a critical reservoir that stabilizes the informational temperature of the field.

The analysis of the entropy–energy ratio Q^{eff} further clarifies this structure. Stable concepts cluster around $Q^{\mathrm{eff}} \simeq 2$, consistent with a theoretical upper limit $S \leq \beta \beta_{\mathrm{c}} E$, analogous to the Bekenstein bound[48] or the Hagedorn scaling[49], where entropy and energy are linearly constrained by a system–specific constant β_{c}. This stability plateau identifies a regime of maximal entropy per unit of informational energy, a point of efficient dissipation where disorder and organization are optimally balanced. Deviations above or below this plateau correspond to under– and over–production of entropy, reflecting adaptive transitions or structural reorganization in semantic space. The emergence of this empirical limit suggests that knowledge systems operate near a critical energy–entropy capacity determined by the finite phase–space volume of accessible information channels k.

Within this framework, the decomposition of irreversible work using the Hatano–Sasa formalism provides a natural quantitative link between microscopic textual fluctuations and macroscopic conceptual order. When the empirical distribution $p_t(k)$ is actively driven through the control parameters (β_t, λ_t), the non–adiabatic entropy production ΔS_{na} quantifies the informational cost of such interventions. The total entropy production remains non–negative because the excess (driving) term ΔS_{ex} compensates for transient increases in the residual information R. Thus, apparent violations of the second law, such as those suggested by Maxwell's paradox, are resolved by explicitly accounting for the information work performed by the "demon" – whether human, algorithmic or collective – during semantic reorganization.

Entropy in this context acquires a dual meaning. The mesoscopic entropy $S_{\mathrm{meso}}[p]$ measures the uncertainty of textual realizations, while the residual entropy $R = D_{\mathrm{KL}}(p \| \pi_\theta)$ quantifies the distance from the instantaneous equilibrium state $\pi_\theta(k)$ on the Maximum Entropy manifold defined by sufficient statistics $\theta = (\beta, \lambda)$. Because R decreases monotonically under coarsegraining, it provides an invariant ordering of concept states by informational distance. Derived quantities such as the entropy–energy coherence $Q^{\mathrm{eff}} = S_{\mathrm{meso}}/(U - \mu N)$ and its stability form $Q^{\mathrm{eff}} = 3/2\beta$ serve as coarse–graining–invariant order parameters that reflect global stability in the informational manifold.

The residual–information ratio ρ_R further distinguishes three characteristic regimes of conceptual dynamics: $\rho_R = 1$ corresponds to near–stationary maintenance, where $\Delta R \simeq 0$; $\rho_R = 0.5$ marks a balanced

exchange between information loss and entropy production under weak driving; and $\rho_R = 0$ identifies purely dissipative transitions with complete structural degradation.

The results thus support three operational principles of an emerging *physical theory of information*: (i) every subsystem interacting with an informational reservoir is characterized by conjugate variables (T, μ) and extensive quantities (U, N); (ii) its non–equilibrium evolution satisfies the extended second law $W_{\mathrm{irr}} = T\,\Delta S_{\mathrm{tot}} \geq 0$; and (iii) for finite systems, the entropy–energy ratio is bounded as $Q^{\mathrm{eff}} \leq \beta\beta_{\mathrm{c}}$, marking the buffered regime where entropy production and information dissipation are balanced. In this sense, the evolution of scientific concepts offers an empirical realization of Maxwell's program for a physical theory of information, one that unifies the statistical mechanics of matter and meaning.

Finally, the framework naturally extends from individual concepts to entire semantic networks. Each concept represents a node whose thermodynamic state is coupled to the network's topology. As a node's thermodynamic length decreases – signaling equilibration – the structural information encoded in its connections is expected to increase. This interplay points toward a new class of *information–thermodynamic uncertainty relations* that link local informational uncertainty to the energetic cost of increasing mutual information with neighboring nodes and, ultimately, with the global network structure. A promising theoretical approach for describing this behavior is the minimization of the Bethe free–energy functional[58], which governs equilibrium configurations in complex networks and probabilistic graphical models. We conjecture that evolving knowledge networks self–organize toward configurations that minimize the Bethe free energy (maximize the nodes entropy and minimize mutual information) under informational driving, thereby balancing local entropy reduction with global structural coherence. Our recent results, reported elsewhere, indicate that equilibrium concepts constitute locally Euclidean cores—regions of minimal curvature within the broader curved information manifold that represents each topic[59][60]. Exploring this connection between thermodynamic node states, network geometry, and topological optimization represents a key next step in extending the present framework from individual node dynamics to the collective thermodynamics of knowledge networks.

In summary, the proposed thermodynamic framework bridges microscopic (textual) dynamics with macroscopic (conceptual) organization, demonstrating that knowledge production follows measurable thermodynamic regularities. The coexistence of equilibrium and nonequilibrium concept populations, the presence of a system–specific critical temperature, and the emergence of efficiency plateaus collectively indicate that the evolution of scientific ideas mirrors the behavior of finite self–organized critical systems. This perspective not only deepens our understanding of the informational mechanics of scientific

communication, but also provides a general methodology for quantifying stability, adaptation, and dissipation across complex symbolic systems from scientific discourse and innovation processes to financial, technological, and biological ecosystems.

Appendix A. Derivation of the irreversible work identity (system reference frame)

For an open system exchanging heat Q, work W, and particles N with its environment, the first law reads

$$dE = \delta Q + \delta W_{\mathrm{mech}} + \mu\, dN, \tag{25}$$

where δW_{mech} is the *mechanical* work done on the system to reorganize the empirical coarse-grained distribution, $\mu\, dN$ is a work done on the system to add new logical particles. The non-equilibrium second law decomposes the total entropy change as

$$dS = \frac{\delta Q}{T} + dS_{\mathrm{i}}, \qquad dS_{\mathrm{i}} \geq 0, \qquad dS_e \equiv \frac{\delta Q}{T}, \tag{26}$$

where dS_{i} is the entropy production and dS_e represents an entropy flow - a reversible contribution from the heat flow δQ.

The entropy production dS_i between empirical $p(t)$ and time dependent Gibbs form reference state $\pi(t)$ is defined as

$$\dot{S}_{\mathrm{i}}(t) = -\frac{d}{dt}\, D_{\mathrm{KL}}\big(p(t) \,\|\, \pi(t)\big) \;+\; \dot{S}_{\mathrm{ex}}[p \,\|\, \pi](t), \qquad \dot{S}_{\mathrm{ex}}[p \,\|\, \pi](t) = -\sum_i p_i(t)\, \partial_t \ln \pi_i(t). \tag{27}$$

where the time dependence of the reference state is a source of the *excess* contribution $\dot{S}_{ex}$.

Introducing the grand potential Φ as a non-equilibrium open system free energy

$$\Phi = E - TS - \mu N$$

and differentiating gives:

$$d\Phi = dE - T\, dS - S\, dT - \mu\, dN - N\, d\mu. \tag{28}$$

Substituting the first and second laws eliminates δQ:

$$\begin{aligned} d\Phi &= (\delta Q + \delta W_{\mathrm{mech}} + \mu\, dN) - T\left(\frac{\delta Q}{T} + dS_{\mathrm{i}}\right) - S\, dT - \mu\, dN - N\, d\mu \\ &= \delta W_{\mathrm{mech}} - T\, dS_{\mathrm{i}} - S\, dT - N\, d\mu. \end{aligned}$$

Hence, we have:

$$T\, dS_{\mathrm{i}} = \delta W_{\mathrm{mech}} - d\Phi - S\, dT - N\, d\mu \geq 0, \tag{29}$$

which is an exact differential identity for the second law of thermodynamics expressed through the non-equilibrium grand potential Φ.

Irreversible work decomposition. We now assume that the reference state is IFP state of a systems mesostate. In this case, the free energy for the grand potential Φ from Eq. (9) from the main text of the paper, assuming time dependence $(S(t), R(t), T(t), \mu(t))$, satisfies the relation:

$$\Phi = \Phi_{\mathrm{IFP}}\,(T, \mu) + T\,R, \qquad S_{\mathrm{IFP}} = S + R. \tag{30}$$

Differentiating yields

$$d\Phi = d\Phi_{IFP} + T\,dR + R\,dT.$$

Substituting this into Eq. (29) gives

$$T\,dS_{\mathrm{i}} = \delta W_{\mathrm{mech}} - d\Phi_{\mathrm{IFP}} - T\,dR - R\,dT - S\,dT - N\,d\mu. \tag{31}$$

Integrating from t_i to t_f gives

$$\int_{t_i}^{t_f} T\,dS_{\mathrm{i}} = W_{\mathrm{mech}} - \Delta\Phi_{\mathrm{IFP}} - \int_{t_i}^{t_f} T\,dR - \int_{t_i}^{t_f} R\,dT - \int_{t_i}^{t_f} S\,dT - \int_{t_i}^{t_f} N\,d\mu. \tag{32}$$

If the system evolves quasistatically along the equilibrium manifold ($S_{\mathrm{i}} = 0$, $R = 0$), Eq. (32) reduces to the definition of the reversible work performed along the same protocol:

$$W_{\mathrm{rev}} = \Delta\Phi_{\mathrm{IFP}} + \int_{t_i}^{t_f} S_{\mathrm{IFP}}\,dT + \int_{t_i}^{t_f} N_{\mathrm{IFP}}\,d\mu. \tag{33}$$

Subtracting Eq. (33) from the general case, we obtain the non-equilibrium irreversible work:

$$\begin{aligned} W_{\mathrm{irr}} &\equiv W_{\mathrm{mech}} - W_{\mathrm{rev}} \\ &= \int_{t_i}^{t_f} T\,dS_{\mathrm{i}} + \int_{t_i}^{t_f} T\,dR + \int_{t_i}^{t_f} \big(R + S - S_{\mathrm{IFP}}\big)\,dT + \int_{t_i}^{t_f} \big(N - N_{\mathrm{IFP}}\big)\,d\mu \\ &= \int_{t_i}^{t_f} T\,dS_{\mathrm{i}} + \int_{t_i}^{t_f} T\,dR = T\Delta S_i + T\,\Delta R. \end{aligned}$$

The Eq. [eq:w_irr_general] is exactly the iso-(T, μ)) form derived by Esposito and Van den Broeck [4]:

$$W_{\mathrm{irr}} = T\,\Delta S_{\mathrm{i}} + T\,\Delta R. \tag{34}$$

clearly identifies the total irreversible work as the sum of two contributions: the production of thermodynamic entropy, $T\,\Delta S_{\mathrm{i}}$, and the informational term, $T\,\Delta R$, associated with the maintenance or reorganization of the non-equilibrium structure of the system.

Appendix B. Residual Entropy and Entropy Production under Instantaneous Fixed-Point Reference

In this appendix we demonstrate that, when the reference distribution is chosen as the *instantaneous fixed point* (IFP) of the system, the time derivative of the residual entropy equals the negative of the entropy production rate:

$$\dot{R}(t) = -\dot{S}_i(t). \tag{35}$$

Let $p_i(t)$ denote the empirical (mesoscopic) probability of observing the microstate i at time t, corresponding in the main text to the document–level frequency distribution $p(k,t)$ defined in Eq. (1). The *instantaneous fixed point* (IFP) or *macrostate* of the system is the distribution that maximizes the Shannon entropy $S_{\text{macro}}(t) = -\sum_i \pi_i(t) \ln \pi_i(t)$ under the current empirical constraints $\langle f_j \rangle_{p(t)} = \langle f_j \rangle_{\pi(t)}$. This constrained maximization yields an exponential–family form (cf. Eqs. 3–4 in the main text):

$$\pi_i(t) = \frac{1}{Z(t)} \exp\left[-\sum_j \theta_j(t) f_j(i)\right], \qquad Z(t) = \sum_i \exp\left[-\sum_j \theta_j(t) f_j(i)\right], \tag{36}$$

where the Lagrange multipliers $\theta_j(t)$ (identified in the main text as $\beta(t)$ and $\lambda(t)$) are determined at each instant by the empirical moments $\langle f_j \rangle_{p(t)}$.

The *residual entropy*—the informational distance between the empirical distribution and its instantaneous MaxEnt reference—is the Kullback–Leibler divergence (cf. Eq. (8) in the main text):

$$R(t) = D_{\text{KL}}(p(t) \,\|\, \pi(t)) = \sum_i p_i(t) \, \ln \frac{p_i(t)}{\pi_i(t)} \geq 0. \tag{37}$$

The equality $R = 0$ occurs only when the mesoscopic state coincides with its IFP, $p(t) = \pi(t)$, that is, when the system is locally in equilibrium with respect to the chosen constraints.

Taking the time derivative of Eq. (37) gives

$$\begin{aligned} \dot{R}(t) &= \sum_i \dot{p}_i \ln \frac{p_i}{\pi_i} + \sum_i p_i \, \frac{d}{dt}\left[\ln \frac{p_i}{\pi_i}\right] \\ &= \sum_i \dot{p}_i \ln \frac{p_i}{\pi_i} + \sum_i p_i \left(\frac{\dot{p}_i}{p_i} - \frac{\dot{\pi}_i}{\pi_i}\right). \end{aligned}$$

The first sum in the second term vanishes because the probabilities are normalized, $\sum_i \dot{p}_i = 0$. Hence,

$$\dot{R}(t) = \sum_i \dot{p}_i \ln \frac{p_i}{\pi_i} - \sum_i p_i \, \frac{\dot{\pi}_i}{\pi_i}. \tag{38}$$

From Eq. (3) we have $\ln \pi_i = -\ln Z - \sum_j \theta_j f_j(i)$, so that

$$\frac{\dot{\pi}_i}{\pi_i} = -\partial_t \ln Z - \sum_j \dot{\theta}_j \, f_j(i). \tag{39}$$

Taking the expectation value with respect to the *empirical* distribution p_i:

$$\sum_i p_i \, \frac{\dot{\pi}_i}{\pi_i} = -\partial_t \ln Z - \sum_j \dot{\theta}_j \, \langle f_j \rangle_p.$$

For an exponential-family distribution, the partition function satisfies $\partial_{\theta_j} \ln Z = -\langle f_j \rangle_\Pi$, so that $\partial_t \ln Z = \sum_j \partial_{\theta_j} \ln Z \, \dot{\theta}_j = -\sum_j \dot{\theta}_j \, \langle f_j \rangle_\Pi$. Substituting this into Eq. [eq:mean_dlnPi] gives

$$\sum_i p_i \, \frac{\dot{\pi}_i}{\pi_i} = -\sum_j \dot{\theta}_j \left(\langle f_j \rangle_p - \langle f_j \rangle_\Pi \right).$$

By definition of the instantaneous fixed point, these expectation values coincide ($\langle f_j \rangle_p = \langle f_j \rangle_\Pi$), and therefore

$$\sum_i p_i \, \frac{\dot{\pi}_i}{\pi_i} = 0. \tag{40}$$

With Eq. (40), the residual-entropy rate (38) reduces to

$$\dot{R}(t) = \sum_i \dot{p}_i(t) \, \ln \frac{p_i(t)}{\pi_i(t)}. \tag{41}$$

For a continuous-time Markov process with transition rates W_{ij}, the entropy production rate is defined as

$$\dot{S}_{\mathrm{i}}(t) = \frac{1}{2} \sum_{i,j} J_{ij}(t) \, \ln \frac{p_i(t) W_{ij}}{p_j(t) W_{ji}}, \quad J_{ij} = p_i W_{ij} - p_j W_{ji}. \tag{42}$$

If the transition rates satisfy detailed balance with respect to the instantaneous reference distribution $\pi_i(t)$,

$$\pi_i(t) \, W_{ij}(t) = \pi_j(t) \, W_{ji}(t),$$

then the right-hand side of Eq. (42) can be rewritten as

$$\dot{S}_{\mathrm{i}}(t) = -\sum_i \dot{p}_i(t) \, \ln \frac{p_i(t)}{\pi_i(t)}.$$

Comparing with Eq. (41) immediately yields the desired identity

$$\dot{R}(t) = -\,\dot{S}_{\mathrm{i}}(t). \tag{43}$$

Equation [eq:dRdt_eq_Sprod] shows that when the reference state is the instantaneous MaxEnt fixed point $\pi(t)$ (determined self-consistently from the data at each time), the residual entropy $R(t)$ decreases exactly at the rate at which the entropy is produced. In fact, the reference state need not be the IFP of the empirical

mesostate, the equation (41) holds when $\dot{\pi} = 0$ and its temperature and chemical potential remained constant ($\dot{\theta}_j = 0$) for the reference state. To see this, we need to compare equations (41) and (27).

In both cases, the system relaxes monotonically toward π, and the relative entropy $R(t)$ plays the role of a Lyapunov function:

$$\dot{R}(t) \leq 0, \qquad \dot{S}_{\mathrm{i}}(t) \geq 0.$$

The identification of R as a measure of "informational distance from equilibrium" justifies its interpretation as an internal measure of the system's nonequilibrium organization, and explains why, under IFP dynamics, entropy production precisely quantifies the rate of information dissipation.

Appendix C. Dynamic Efficiency and Work Decomposition in Concept Evolution

To quantify the efficiency of concept evolution as a non-equilibrium process, we consider the system (a scientific concept) interacting with an effectively isothermal informational reservoir at temperature T_{ref}, representing the statistical background of its topical environment. At discrete times t, the concept is described by its empirical mesostate $p_t(k)$ and the corresponding instantaneous fixed point (IFP) $\pi_t(k)$ obtained by maximum entropy fitting under constraints $\langle k \rangle_{p_t} = \langle k \rangle_{\pi_t}$ and $\langle \ln k \rangle_{p_t} = \langle \ln k \rangle_{\pi_t}$. The non-equilibrium potential is defined as $\phi_t(k) = -\ln \pi_t(k)$.

Discrete Hatano–Sasa decomposition

The Hatano–Sasa equality [37][47] extends the fluctuation theorems to transitions between non-equilibrium steady states (NESS) or IFPs. For a discrete-time trajectory $p_t \to p_{t+1}$, we define the excess functional

$$\widehat{Y}_{t\to t+1} = \sum_k p_t(k) \left[\phi_{t+1}(k) - \phi_t(k)\right] = \sum_k p_t(k) \, \ln \frac{\pi_t(k)}{\pi_{t+1}(k)}, \tag{44}$$

which satisfies $\langle e^{-\widehat{Y}} \rangle = 1$ and therefore $\langle \widehat{Y} \rangle \geq 0$. The total entropy production accumulated over a process consists of two additive contributions:

$$\Delta S_{\mathrm{tot}} = \Delta S_{\mathrm{na}} + \Delta S_{\mathrm{a}}, \tag{45}$$

where

$$\Delta S_{\mathrm{na}} = \underbrace{\Delta R}_{D_{\mathrm{KL}}(p_f\|\pi_f)-D_{\mathrm{KL}}(p_i\|\pi_i)} + \sum_t \widehat{Y}_{t\to t+1} \qquad \text{(non-adiabatic, excess)},$$

$$\Delta S_{\mathrm{a}} = \Delta S_{\mathrm{tot}} - \Delta S_{\mathrm{na}} \geq 0 \qquad \text{(adiabatic, housekeeping)}.$$

Here ΔR is the change in residual (informational) entropy, quantifying how the empirical distribution p_t approaches or departs from its instantaneous fixed point π_t. The first term, ΔS_{na}, represents the irreversible entropy production associated with parameter driving or adaptation of the IFP, while the second term, ΔS_{a}, measures the steady dissipation required to sustain non-equilibrium currents even when the parameters are fixed.

In an isothermal process at temperature T_{ref}, the dissipated irreversible work equals the total entropy production multiplied by T_{ref}:

$$W_{\mathrm{tot}} = T_{\mathrm{ref}}\,\Delta S_{\mathrm{tot}} = T_{\mathrm{ref}}\big(\Delta S_{\mathrm{na}} + \Delta S_{\mathrm{a}}\big) = W_{\mathrm{ex}} + W_{\mathrm{hk}}, \tag{46}$$

where

$$W_{\mathrm{ex}} = T_{\mathrm{ref}}\,\Delta S_{\mathrm{na}}, \qquad W_{\mathrm{hk}} = T_{\mathrm{ref}}\,\Delta S_{\mathrm{a}}.$$

The total dissipated work W_{tot} thus separates into: (i) an *excess work* W_{ex} associated with adaptive changes in the system's IFP (informational "steering"), and (ii) a *housekeeping work* W_{hk} corresponding to the steady dissipation required to maintain the system's non-equilibrium structure.

The reference temperature T_{ref} defines the informational "bath" in contact with the concept.

Mid-point approximation for entropy production estimate In the main text, we distinguish two quantities: the change in *residual entropy* $R = D(p\|p^{\mathrm{eq}})$, which quantifies the instantaneous distance between the empirical state and its equilibrium reference, and the *entropy production* ΔS_{i}, which measures the total irreversible dissipation accumulated along a trajectory. These quantities coincide only for relaxation toward a fixed equilibrium; in general, R is a *state function*, while S_{i} depends on the full path taken.

For empirical data sampled at discrete times t_i and t_f, we approximate the integrated entropy balance of Eq. (26) over a finite interval $\Delta t = t_f - t_i$ as

$$\Delta S = \Delta S_{\mathrm{e}} + \Delta S_{\mathrm{i}}, \qquad \Delta S_{\mathrm{e}} = \int_{t_i}^{t_f} \frac{\delta Q}{T}. \tag{47}$$

The entropy flow ΔS_{e} is evaluated using a midpoint (Stratonovich[61]) approximation of the time-dependent reference distribution $p^{\mathrm{eq}}(t)$, defined by the average bath parameters

$$\beta_* = \tfrac{1}{2}\big[\beta(t_i) + \beta(t_f)\big], \qquad \mu_* = -\,\frac{\lambda(t_i) + \lambda(t_f)}{\beta(t_i) + \beta(t_f)}.$$

For each mesoscopic state k we define the “generalized energy”

$$H(k) = \ln k - \mu_* \, k,$$

so that the entropy flow over the interval is estimated by

$$\Delta S_{\mathrm{e}} \simeq \beta_* \sum_k \left[P_c(k, t_f) - P_c(k, t_i) \right] H(k). \tag{48}$$

This expression follows directly from discretizing the excess term

$$\dot{S}_{\mathrm{ex}}(t) = -\sum_i p_i(t) \, \partial_t \ln p_i^{\mathrm{eq}}(t)$$

replacing the derivative ∂_t by a finite difference evaluated in the bath parameters at the midpoint (T_*, μ_*).

The total entropy production over the interval is then obtained as

$$\Delta S_{\mathrm{i}} = \Delta S - \Delta S_{\mathrm{e}} \geq 0, \tag{49}$$

consistent with the second law. In practice, small negative values due to sampling noise are truncated to zero. Finally, the change in residual entropy

$$\Delta R = R(t_f) - R(t_i) = \left[S_{\mathrm{macro}}(t_f) - S(t_f) \right] - \left[S_{\mathrm{macro}}(t_i) - S(t_i) \right]$$

quantifies the variation of informational mismatch between empirical and equilibrium states.

This midpoint estimator provides a numerically stable and physically consistent way to compute the entropy production and the efficiency of the information-flow directly from empirical frequency distributions $p(k, t)$, while retaining the connection to the continuous-time formulation based on $D(p \| p^{\mathrm{eq}})$ and the Esposito–Seifert decomposition [4][37].

Appendix D. Nonequilibrium Grand Potential Gap Equals $T\,R$ at Fixed (T, μ)

We consider the discrete microstate index $k \in \mathbb{N}$ with “energy”

$$H(k) \;=\; \ln k \;-\; \mu \, k, \qquad \beta \equiv 1/T, \qquad \lambda \equiv \beta\mu. \tag{50}$$

At each time t on a fixed grid, let $p_t(k)$ denote the empirical (nonequilibrium) distribution and let the instantaneous fixed point (IFP) $\pi_t(k)$ be the maximum-entropy (grand-canonical) distribution at the same intensives (T_t, μ_t):

$$\pi_t(k) \;=\; \frac{1}{Z_t} \, e^{-\beta_t H_t(k)} \;=\; \frac{1}{Z_t} \, k^{-\beta_t} e^{-\lambda_t k}, \qquad Z_t \;=\; \sum_{k \geq 1} e^{-\beta_t H_t(k)}. \tag{51}$$

The nonequilibrium grand potential of p at fixed (T,μ) is

$$\Phi[p;T,\mu] \;=\; \big\langle H \big\rangle_p \;-\; T\,S[p] \;=\; \sum_k p_k(\ln k - \mu k) \;-\; T\Big(-\sum_k p_k \ln p_k\Big), \tag{52}$$

and the IFP (equilibrium) grand potential is

$$\Phi_{\mathrm{IFP}}(T,\mu) \;\equiv\; \Phi[\pi;T,\mu] \;=\; -T\ln Z. \tag{53}$$

For any distribution p and its IFP π at the *same* (T,μ),

$$\big(\Phi - \Phi_{\mathrm{IFP}}\big)_{T,\mu} \;=\; T\,R(p\|\pi) \;\geq\; 0, \tag{54}$$

with equality if and only if $p=\pi$ (a.e.).

Proof. Compute the Kullback–Leibler divergence

$$R(p\|\pi) \;=\; \sum_k p_k \ln\frac{p_k}{\pi_k} \;=\; \sum_k p_k \ln p_k \;-\; \sum_k p_k \ln \pi_k. \tag{55}$$

Since $\ln \pi_k = -\beta H(k) - \ln Z$, we have

$$R(p\|\pi) \;=\; \sum_k p_k \ln p_k \;+\; \beta\sum_k p_k H(k) \;+\; \ln Z. \tag{56}$$

Multiplying by T yields

$$T\,R \;=\; T\sum_k p_k \ln p_k \;+\; \sum_k p_k H(k) \;+\; T\ln Z \;=\; \underbrace{\Big(\langle H\rangle_p - T\,S[p]\Big)}_{\Phi[p;T,\mu]} \;-\; \underbrace{\big(-T\ln Z\big)}_{\Phi_{\mathrm{IFP}}(T,\mu)}. \tag{57}$$

Thus $\Phi[p;T,\mu] - \Phi_{\mathrm{IFP}}(T,\mu) = T\,R(p\|\pi) \geq 0$, with an equality iff $R=0$, i.e., $p=\pi$. $\square$

The result (54) requires only that (T,μ) be held fixed; it does *not* assume fixed extensive moments such as $\langle k\rangle$ or $\langle \ln k\rangle$. Differences in these moments between p and π are precisely encoded in $R(p\|\pi)$.

On a discrete time grid $\{t_n\}$ with intensives (T_{t_n},μ_{t_n}) and pairs (p_{t_n},π_{t_n}),

$$\Phi\big(p_{t_n};T_{t_n},\mu_{t_n}\big) \;-\; \Phi_{\mathrm{IFP}}\big(T_{t_n},\mu_{t_n}\big) \;=\; T_{t_n}\,R\big(p_{t_n}\|\pi_{t_n}\big) \;\geq 0 \qquad \text{for each } t_n. \tag{58}$$

Writing

$$\Phi[p;T,\mu] \;=\; \underbrace{\Phi_{\mathrm{IFP}}(T,\mu)}_{\text{equilibrium part}} \;+\; \underbrace{T\,R(p\|\pi)}_{\text{nonequilibrium excess}}, \tag{59}$$

makes explicit that TR is the residual information potential that elevates Φ above its IFP value.

Nomenclature

tf	Term frequency: number of times $k \in \mathbb{Z}^+$ a concept appears in a document.
$N_c(t)$	Number of documents containing concept c up to time t.
$N_c(k, t)$	Number of documents containing c exactly k times up to time t.
$p(k, t)$	Observed probability that concept c is cited k times up to t.
$p_c(\{k\}, t) \equiv p_t$	Mesostate probability mass function at time t.
$\pi^{\text{eq}}(k, t; \beta, \lambda)$	Reference probability mass function at time t (thermal bath).
$\pi(k, t) \equiv \pi_t$	Macrostate PMF or instantaneous fixed point (IFP) of the mesostate p_c.
β	Lagrange multiplier; inverse temperature ($\beta = 1/(k_B T)$).
λ	Lagrange multiplier related to the chemical potential.
μ	Chemical potential ($\mu = -\lambda/\beta$).
k_B	Boltzmann constant (set $k_B = 1$ in numerical computations).
Z	Grand partition function that normalizes the macrostate PMF.
$U = \langle \ln k \rangle$	Internal (information) energy of a concept per document.

doi.org/10.32388/UM6NLZ.3

$N = \langle k \rangle$	Average number of logical particles (concept mentions).
$E = U - \mu N$	The generalized energy function.
S	Mesostate entropy per document derived from $p(k,t)$.
S_{macro}	Macrostate (thermodynamic) entropy per document.
$Q^{\text{eff}} = S/E$	Entropy efficiency.
R	Residual entropy, $R = S_{\text{macro}} - S$.
Φ	Grand canonical potential, $\Phi = U - TS - \mu N$.
ΔR	Change in residual entropy over a finite interval Δt.
TR	Residual (informational) energy — $\Phi - \Phi_{\text{IFP}}$.
C_μ	Heat capacity at constant chemical potential, $C_\mu = (\partial U/\partial T)_\mu$.
C_N	Heat capacity at constant document support, $C_N = (\partial U/\partial T)_N$.
χ_T	Particle-number susceptibility, $\chi_T = (\partial N/\partial \mu)_T$.
α_μ	Thermal expansion coefficient, $\alpha_\mu = (1/N)(\partial N/\partial T)_\mu$.
α_E	Energy–chemical potential coupling coefficient, $\alpha_E = (\partial \langle E \rangle/\partial \mu)_T$.
C_μ^E	Heat capacity at constant chemical potential for effective energy E.
η_{hk}	Housekeeping efficiency, $\eta_{\text{hk}} = \Delta S_a / \Delta S_{\text{tot}}$.
η_{ex}	Driving (adaptive) efficiency, $\eta_{\text{ex}} = \Delta S_{na} / \Delta S_{\text{tot}} = 1 - \eta_{\text{hk}}$.
ρ_R	Residual-information retention ratio, $\rho_R = 1 - [-\Delta R]^+ / \Delta S_{\text{tot}}$.

Statements and Declarations

Funding

The University of Warsaw supported this publication under Priority Research Area V of the “Excellence Initiative—Research University” program.

Conflicts of Interest

The authors declare no conflicts of interest.

Author contributions

Conceptualization, A.C. and B.B.; methodology, A.C.; software, A.C.; validation, A.C.; formal analysis, A.C.; investigation, A.C.; resources, A.C.; data curation, A.C.; writing---original draft preparation, A.C.; writing---review and editing, A.C.; visualization, A.C.; supervision, A.C.; project administration, A.C.; funding acquisition, B.B. All authors have read and agreed to the published version of the manuscript.}

Data Availability

All materials related to the research are available and can be accessed through Zenodo: 10.5281/zenodo.17611701.

Acknowledgments

We would like to acknowledge that this manuscript overlaps with the preprint [62] available on Qeios. The preprint version of this work was previously made available by the authors.

We also extend our gratitude to the University of Warsaw, Center for European Regional and Local Studies (EUROREG), for their valuable support.

References

1. ^*Claude Elwood Shannon. (1948). A mathematical theory of communication. The Bell System Technical Jour nal. 27:379–423.*
2. ^*Edwin Jaynes. (1957). Information theory and statistical mechanics i. Physical Review. 106:620–630. doi:10.1 103/PhysRev.106.620*
3. ^*Sebastian Goldt, Udo Seifert. (2017). Stochastic thermodynamics of learning. Physical Review Letters. 118(1): 010601. doi:10.1103/PhysRevLett.118.010601*
4. a, b, c, d*Massimiliano Esposito, Chris Van Den Broeck. (2011). Second law and landauer principle far from equi librium. EPL (Europhysics Letters). 95:40004. Available from: https://api.semanticscholar.org/CorpusID:39388 312*

5. ^Juan M. R. Parrondo, Jordan M. Horowitz, Takahiro Sagawa. (2015). Thermodynamics of information. Natur e Physics. 11(2):131–139. doi:10.1038/nphys3230
6. ^Manabendra Nath Bera, Andreas Winter, Maciej Lewenstein. Thermodynamics from Information. In: Felix Binder, Luis A. Correa, Christian Gogolin, Janet Anders, Gerardo Adessoeditors. Thermodynamics in the Quan tum Regime.: Cham: Springer International Publishing 2018. pp. 799–820. doi:10.1007/978-3-319-99046-0_33. ISBN 978-3-319-99045-3 978-3-319-99046-0
7. ^Andreas Paglietti. (2023). Why Thermodynamic Entropy and Statistical Entropy are TwoDifferent Physical Quantities. Current Physical Chemistry. 13(3):233–245. doi:10.2174/1877946813666230622161503
8. ^David Wallace. (2021). Philosophy of physics: A very short introduction. Oxford: Oxford University Press.
9. ^Ariel Caticha. (2021). Entropy, Information, and the Updating of Probabilities. Entropy. 23(7):895. doi:10.339 0/e23070895
10. a, bXiang Gao, Emilio Gallicchio, Adrian E. Roitberg. (2019). The generalized Boltzmann distribution is the onl y distribution in which the Gibbs-Shannon entropy equals the thermodynamic entropy. The Journal of Chemi cal Physics. 151(3):034113. doi:10.1063/1.5111333
11. ^Rolf Landauer. (1961). Irreversibility and heat generation in the computing process. IBM Journal of Research and Development. 5(3):183–191. doi:10.1147/rd.53.0183
12. ^Leon Brillouin. (1956). Science and information theory. New York: Academic Press.
13. ^Juan M. R. Parrondo. (2023). Thermodynamics of information. Reference Module in Materials Science and Materials Engineering. doi:10.1016/B978-0-323-90800-9.00174-8
14. a, bRoman Prokofyev, Gianluca Demartini, Alexey Boyarsky, Oleg Ruchayskiy, Philippe Cudré-Mauroux. Onto logy-Based Word Sense Disambiguation for Scientific Literature. In: David Hutchison, Takeo Kanade, Josef Ki ttler, Jon M. Kleinberg, Friedemann Mattern, et al.editors. Advances in Information Retrieval.: Berlin, Heidelbe rg: Springer Berlin Heidelberg 2013. pp. 594–605. doi:10.1007/978-3-642-36973-5_50. ISBN 978-3-642-36972- 8 978-3-642-36973-5
15. ^John Dagdelen, Alexander Dunn, Sanghoon Lee, Nicholas Walker, Andrew S. Rosen, et al. (2024). Structured i nformation extraction from scientific text with large language models. Nature Communications. 15(1):1418. d oi:10.1038/s41467-024-45563-x
16. a, b, c, dHuan-Kai Peng, Ying Zhang, Peter Pirolli, Tad Hogg. (2012). Thermodynamic Principles in Social Colla borations. ArXiv. doi:10.48550/ARXIV.1204.3663
17. ^Andrea Martini, Artem Lutov, Valerio Gemmetto, Andrii Magalich, Alessio Cardillo, et al. ScienceWISE: Topic Modeling over Scientific Literature Networks. arXiv 2016.

18. ^Vasyl Palchykov, Valerio Gemmetto, Alexey Boyarsky, Diego Garlaschelli. (2016). Ground truth? Concept-based communities versus the external classification of physics manuscripts. EPJ Data Science. 5(1):28. doi:10.1140/epjds/s13688-016-0090-4

19. ^Serhii Brodiuk, Vasyl Palchykov, Yurij Holovatch. (2020). Embedding technique and network analysis of scientific innovations emergence in an arXiv-based concept network. ArXiv. doi:10.48550/ARXIV.2003.10289

20. a, b, cAndrea Martini, Alessio Cardillo, Paolo De Los Rios. (2018). Entropic selection of concepts unveils hidden topics in documents corpora. ArXiv. Available from: https://arxiv.org/abs/1705.06510

21. ^Vasyl Palchykov, M. Krasnytska, Olesya Mryglod, Yu Holovatch. (2021). Network of scientific concepts: Empirical analysis and modeling. Advances in Complex Systems. 24. doi:10.1142/S0219525921400014

22. ^T. M. Cover, J. A. Thomas. (2012). Elements of information theory. Wiley. Available from: https://books.google.pl/books?id=VWq5GG6ycxMC. ISBN 9781118585771

23. ^Ariel Caticha, Ali Mohammad-Djafari, Jean-François Bercher, Pierre Bessiere. (2011). Entropic inference. In: AIP conference proceedings.: AIP. doi:10.1063/1.3573619

24. a, bPhilipp Strasberg, Massimiliano Esposito. (2019). Non-markovianity and negative entropy production rates. Physical Review E. 99(1):012120. doi:10.1103/PhysRevE.99.012120

25. ^T. L. Hill. (1986). An introduction to statistical thermodynamics. Dover Publications. (Addison-wesley series in chemistry). Available from: https://books.google.pl/books?id=pX4yxOHnWg8C. ISBN 9780486652429

26. ^Carlo Sparaciari, Jonathan Oppenheim, Tobias Fritz. (2017). Resource theory for work and heat. Phys Rev A. 96:052112. doi:10.1103/PhysRevA.96.052112

27. ^Manabendra Bera, Arnau Riera, Maciej Lewenstein, Andreas Winter. (2017). Thermodynamics as a consequence of information conservation. Quantum. 3. doi:10.22331/q-2019-02-14-121

28. ^Gavin E. Crooks. (2007). Measuring thermodynamic length. Physical Review Letters. 99(10):100602. doi:10.1103/PhysRevLett.99.100602

29. ^George Ruppeiner. (1995). Riemannian geometry in thermodynamic fluctuation theory. Reviews of Modern Physics. 67(3):605–659. doi:10.1103/RevModPhys.67.605

30. ^Riccardo Rao, Massimiliano Esposito. (2016). Nonequilibrium thermodynamics of chemical reaction networks: Wisdom from stochastic thermodynamics. Physical Review X. 6(4):041064. doi:10.1103/PhysRevX.6.041064

31. ^Artem Chumachenko. Information geometry of scientific topics.

32. ^Hong Qian. (2001). Relative entropy: Free energy associated with equilibrium fluctuations and nonequilibrium deviations. Physical Review E. 63(4):042103. doi:10.1103/PhysRevE.63.042103

33. ^Suriyanarayanan Vaikuntanathan, Christopher Jarzynski. (2009). Dissipation and lag in irreversible proces ses. EPL (Europhysics Letters). 87:60005. doi:10.1209/0295-5075/87/60005

34. ^Juan M. R. Parrondo, Jordan M. Horowitz, Takahiro Sagawa. (2015). Thermodynamics of information. Natur e Physics. 11(2):131–139. doi:10.1038/nphys3230

35. ^J. Schnakenberg. (1976). Network theory of microscopic and macroscopic behavior of master-equation syste ms. Rev Mod Phys. 48:571–585.

36. ^Imre Csiszár. (1967). Information-type measures of difference of probability distributions and indirect obser vation. Studia Sci Math Hungar. 2:299–318.

37. a, b, c, dMassimiliano Esposito, Christian Van den Broeck. (2010). Three detailed fluctuation theorems. Physica l Review Letters. 104(9):090601. doi:10.1103/PhysRevLett.104.090601

38. ^Udo Seifert. (2012). Stochastic thermodynamics, fluctuation theorems and molecular machines. Rep Prog P hys. 75:126001.

39. ^K. Binder. (1987). Finite size effects on phase transitions. Ferroelectrics. 73(1):43–67. doi:10.1080/0015019870 8227908

40. ^Michael Fisher. Scaling, university and renormalization group theory. In: Lect Notes Phys. 2006. pp. 1–139. d oi:10.1007/3-540-12675-9_11. ISBN 978-3-540-12675-1

41. ^Riccardo Rao, Massimiliano Esposito. (2016). Nonequilibrium thermodynamics of chemical reaction networ ks: Wisdom from stochastic thermodynamics. Phys Rev X. 6:041064. doi:10.1103/PhysRevX.6.041064

42. ^Matteo Polettini, Massimiliano Esposito. (2014). Irreversible thermodynamics of open chemical networks. I. Emergent cycles and broken conservation laws. The Journal of Chemical Physics. 141(2):024117. doi:10.1063/1.4 886396

43. ^Hong Qian. (2007). Phosphorylation energy hypothesis: Open chemical systems and their biological functio ns. Annual Review of Physical Chemistry. 58:113–142. doi:10.1146/annurev.physchem.58.032806.104550

44. ^H. E. Stanley. (1971). Introduction to phase transitions and critical phenomena. Oxford University Press. (Inte rnational series of monographs on physics). Available from: https://books.google.pl/books?id=C3BzcUxoaNk C. ISBN 9780195053166

45. ^Michael E. Fisher. (1974). The renormalization group in the theory of critical behavior. Reviews of Modern P hysics. 46(4):597–616. doi:10.1103/RevModPhys.46.597

46. ^Mikhail A. Anisimov. (1991). Critical phenomena in liquids and liquid crystals. In. Available from: https://api. semanticscholar.org/CorpusID:93093498

47. ^a, ^b, ^cTakahiro Hatano, Shin-ichi Sasa. (2001). Steady-state thermodynamics of langevin systems. Physical Review Letters. 86(16):3463–3466. doi:10.1103/PhysRevLett.86.3463

48. ^a, ^bJ. D. Bekenstein. (1981). Universal upper bound on the entropy-to-energy ratio for bounded systems. Physical Review D. 23(2):287–298. doi:10.1103/PhysRevD.23.287

49. ^a, ^bR. Hagedorn. (1965). Statistical thermodynamics of strong interactions at high energies. Supplemento al Nuovo Cimento. 3:147–186.

50. ^S. C. Frautschi. (1971). Statistical bootstrap model of hadrons. Physical Review D. 3(10):2821–2834. doi:10.1103/PhysRevD.3.2821

51. ^F. Schlögl. (1972). Chemical reaction models for non-equilibrium phase transitions. Z Physik. 253:147–161. doi:10.1007/BF01379769

52. ^G. Nicolis, I. Prigogine. (1977). Self-organization in nonequilibrium systems. Wiley.

53. ^N. G. van Kampen. (2007). Stochastic processes in physics and chemistry. 3rd ed. Elsevier.

54. ^M. E. Fisher, M. N. Barber. (1972). Scaling theory for finite-size effects in the critical region. Phys Rev Lett. 28:1516–1519. doi:10.1103/PhysRevLett.28.1516

55. ^K. Binder. (1981). Finite size scaling analysis of ising model block distribution functions. Z Phys B. 43:119–140. doi:10.1007/BF01293604

56. ^V. Privmaneditor. (1990). Finite size scaling and numerical simulation of statistical systems. World Scientific.

57. ^N. Goldenfeld. (1992). Lectures on phase transitions and the renormalization group. Addison–Wesley.

58. ^Anand Rangarajan, Alan L. Yuille. (2001). MIME: Mutual information minimization and entropy maximization for bayesian belief propagation. In: T. Dietterich, S. Becker, Z. Ghahramanieditors. Advances in neural information processing systems.: MIT Press. Available from: https://proceedings.neurips.cc/paper_files/paper/2001/file/f1981e4bd8a0d6d8462016d2fc6276b3-Paper.pdf

59. ^Shun-ichi Amari, Atsumi Ohara, Hiroshi Matsuzoe. (2012). Geometry of deformed exponential families: Invariant, dually-flat and conformal geometries. Physica A: Statistical Mechanics and its Applications. 391(18):4308–4319. doi:https://doi.org/10.1016/j.physa.2012.04.016

60. ^Bradley Efron. (1978). The geometry of exponential families. The Annals of Statistics. 6(2):362–376. Available from: http://www.jstor.org/stable/2958883

61. ^R. L. Stratonovich. (1966). A new representation for stochastic integrals and equations. SIAM Journal on Control. 4(2):362–371. doi:10.1137/0304028

62. ^Artem Chumachenko and Brett Buttliere. “Quantifying Knowledge Evolution With Thermodynamics: A Data-Driven Study of Scientific Concepts”. In: Qeios (Oct. 2024). issn: 2632-3834. doi: 10.32388/UM6NLZ.2. url: htt

ps://doi.org/10.32388/UM6NLZ.2

Declarations

Funding: This study supported by the University of Warsaw.

Potential competing interests: No potential competing interests to declare.